Multiple Turbine Flow Distribution Control using Intelligent Controller in Mini Hydro Power Plant.

U.L.D.V Deshapriya

(188658K)

Degree of Master of Science in Industrial Automation

Department of Electrical Engineering

Faculty of Engineering

University of Moratuwa

Sri Lanka

December 2021

Multiple Turbine Flow Distribution Control using Intelligent Controller in Mini Hydro Power Plant.

U L D V Deshapriya

(188658K)

Thesis/Dissertation submitted in partial fulfillment of the requirements for the degree Master of Science in Industrial Automation

Department of Electrical Engineering

Faculty of Engineering

University of Moratuwa

Sri Lanka

December 2021

DECLARATION

I declare that this is my own work and this thesis/dissertation does not incorporate without acknowledgement any material previously submitted for a Degree or Diploma

in any other University or Institute of higher learning and to the best of my knowledge and belief it does not contain any material previously published or written by another person except where the acknowledgement is made in the text. I retain the right to use this content in whole or part in future works (such as articles or books).

Signature: Date:

………………………..

U L D V Deshapriya

The above candidate has carried out research for the Masters thesis under my supervision. I confirm that the declaration made above by the student is true and correct.

Name of the supervisor: Prof. A.G.B.P Jayasekara

Signature of the supervisor: Date:

………………………..

ACKNOWLEDGEMENT

I would like to express my sincere gratitude to my project supervisor, Prof. A.G.B.P Jayasekara in the Department of Electrical Engineering at the University of Moratuwa, for his continuous support in my M.Sc. studies and research. Their patience, motivation, enthusiasm, and guidance have been the source of inspiration behind my success.

I would also like to thank academic staff members of the Department of Electrical Engineering for their encouragement and insightful comments during progress review sessions.

I would like to express my sincere gratitude to Resus Energy PLC for the support extended to me. In particular, I thank the power plant supervisor and the staff of Moragaha Oya power plant for their dedication.

I would like to convey my sincere gratitude to my wife Buddhini Anushika and family members who helped me in numerous ways to achieve my targets all the time.

Last but not least, I would like to thank my brother Tharindu Sampath for his excellent craftsmanship in the design and fabrication of all hardware components installed in the power plant.

ABSTRACT

Mini hydropower plants have been located at relatively small streams such streams often found upstream of a large river system. With a small catchment and high runoff, those stream parameters such as flow, debris content and water purity are highly dynamic with seasonal intense rainfall.

To generate maximum electricity from river available flow, mini hydropower plants are equipped with multiple turbines. Thus, different flow combinations can be used to harvest maximum energy. The Present flow distribution control technique consists of a PID loop and a pre-tuned flow distribution table which allocates flow to each turbine by changing wicket gate opening depending upon available river flow.

But as a result of variable stream parameters, water density and penstock friction losses will drastically change and therefore a flow distribution combination given by the existing controller may not be the optimum combination for the given moment. with alternating upstream rainfalls, most mini hydropower plants are not able to reach maximum design capacity even with 100% flow until clear water appears in the river.

This research aims to introduce an artificial neuron network based intelligent controller which will measure flow variables and update the flow distribution table frequently ensuring optimum flow distribution and maximum power generation.

"Moragaha Oya" mini hydropower plant located in Kandy district, Sri Lanka is selected as the test site for this research. Required additional hardware has been installed for the water quality and rainfall measurements. Developed intelligent controller with data collection and training software has been installed in power plant control computer enabling the update of flow distribution table. The intelligent controller has been trained and performance validation completed.

A significant improvement of total output power has been obtained during performance validation, especially during the flow conditions where the existing controller could not obtain the optimum flow condition. the maximum output power increment is recorded as 3% of the previous maximum output power. By using energy harvest data of 47 days and rainfall data of the last 4 years, a 2% increment of annual energy harvest was also predicted during performance validation. Required further developments were also identified.

The findings of this research may very important to renewable energy developers to optimize their powerplant yield.

TABLE OF CONTENTS

LIST OF FIGURES

LIST OF TABLES

LIST OF ABBREVIATIONS

Abbreviation	Description
NCRE	- Non-Conventional Renewable Energy
IPP	- Independent Power Producers
IRR	- Internal Rate of Return
HV	- High Voltage
PLC	- Programmable Logic Controller
SCADA	- Supervisory Control and Data Acquisition
HMI	- Human Machine Interface
MV	- Medium Voltage
PID	- Proportional Integral Derivative
3D	-Three Dimensional
PC	- Personal Computer
ANN	- Artificial Neural Network
GUI	- Graphical User Interface
TDS	- Total Dissolved solids
TSS	- Total Suspended solids
RMS	- Root Mean Square
NTU	- Nephelometric Turbidity Units
CPU	- Central Processing Unit
AC	- Alternating Current
DC	- Direct Current
LED	- Light Emitting Diode
TCP	- Transmission Control Protocol
RAM	- Random Access Memory
yr	- Year

hr - Hour

LIST OF APPENDICES

OBJECTIVE

“The specific objective of this research is to identify the relationship between water quality parameters and the power loss and develop an intelligent controller capable of distributing water flow between turbines based on identified inputs that ensure maximum power generation at an available flow.”

1. INTRODUCTION

None conventional renewable energy (NCRE) generation plays a vital role in the world energy mix. When it comes to the specific area of electricity generation, nearly 11% of the world's electricity generation is achieved by NCRE technologies. Also, in the Sri Lankan context, NCRE share has been grown up to 18% of the electricity generation mix.

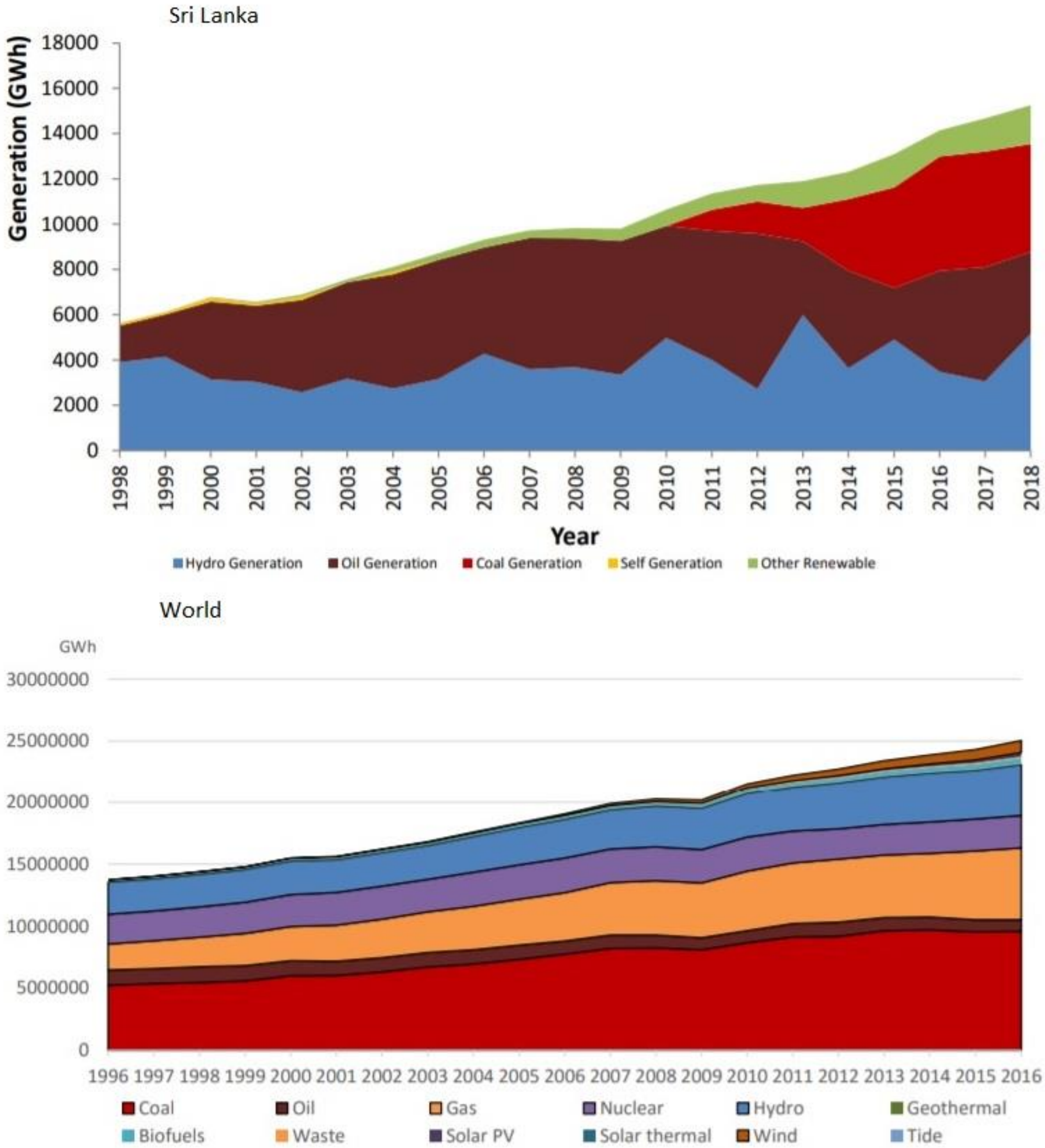

Figure 1: Electricity generation mix world and Sri Lanka.

Currently, a number of NCRE generation methods are being used in Sri Lanka namely Solar PV, wind, biomass, mini-hydro, etc. Figure 1 shows the energy generation mix in Sri Lanka and the World respectively. Being a water-rich country, Sri Lanka has a huge potential for mini-hydro projects, and harnessing a stream for hydroelectric power is a major undertaking for the energy crises and the global issues to go green. According to the government regulations, IPP's are allowed to develop mini-hydropower plants of "built own and operate" basis up to 10 MW of capacity. A number of local companies and individuals are engaged with mini-hydro business and it has proven as a highly profitable business with an average IRR of 14% under present tariff schemes. Nearly 212 mini hydropower plants are operating in Sri Lanka contributing 1,200 GWh of electrical energy annually to the national grid which is about 7.51% of the national electricity consumption.

When it comes to the evolution of the design and construction of mini hydropower plants in Sri Lanka, early known power plants had located at colonial-era tea factories. Those power plants are equipped with primitive control technologies and operated in island mode. But with later developments of the grid-connected embedded generation concept, the Electromechanical component of the power plants with advanced control systems and protections systems were imported as whole packages from countries like the United Kingdom and Germany. Followed by rapid technology acquisition, local companies start to develop their own turbines, generators, control systems, and transformers. Also, they tend to integrations components from various manufacturers around the globe especially Chinese build turbines and generators. In the civil and mechanical engineering design and construction front, Local companies acquire technologies rapidly and start implementing their own weir and penstock designs. Figure 2 shows the stages of construction of a mini hydropower plant in Sri Lanka.

Even with above mentioned matured technical capability, lack of research and developments, lack of detailed design capabilities, poor engineering practices and incomplete environmental impact assessments can be identified as the main drawbacks of this industry. As a result of that, most of these power plants undergo with issues such as inability to reach design capacity, less plant factor due to inaccurate hydrology assessments, frequent breakdowns and so on. This research aims to address such an issue related to mini-hydro industry.

Figure 2: Construction of mini hydro power plant in Sri Lanka (Hulu Ganga mini hydro power plant)

1.1 Overview of mini hydro power plant

Usually, conventional hydropower generation projects are viewed as constructing large dams and reservoirs, longer penstock lines with advanced drilling, constriction of large powerhouses and construction of dedicated HV transmission lines. but available mini hydropower plant construction techniques have helped hydropower generation without large dams, large reservoirs and other expensive infrastructure [16]. In Sri Lanka, there are a number of small streams or running rivers, water installations, irrigation dams, canals, which are tapped to generate power by constructing mini hydropower plants. In these power plants, the existing system and facilities can help in generating power with less investment and less construction time. Also, those techniques help to harvest maximum energy even with highly dynamic flows where small streams often exhibit high flow variation with weather changes. A mini hydropower plant mainly consists of a weir, intake canal, head raise penstock pipeline, powerhouse with hydraulic turbine and generators, control system and switch gears, transformers and a medium or low voltage transmission line. Figure 3 shows the typical layout of a mini hydropower plant.

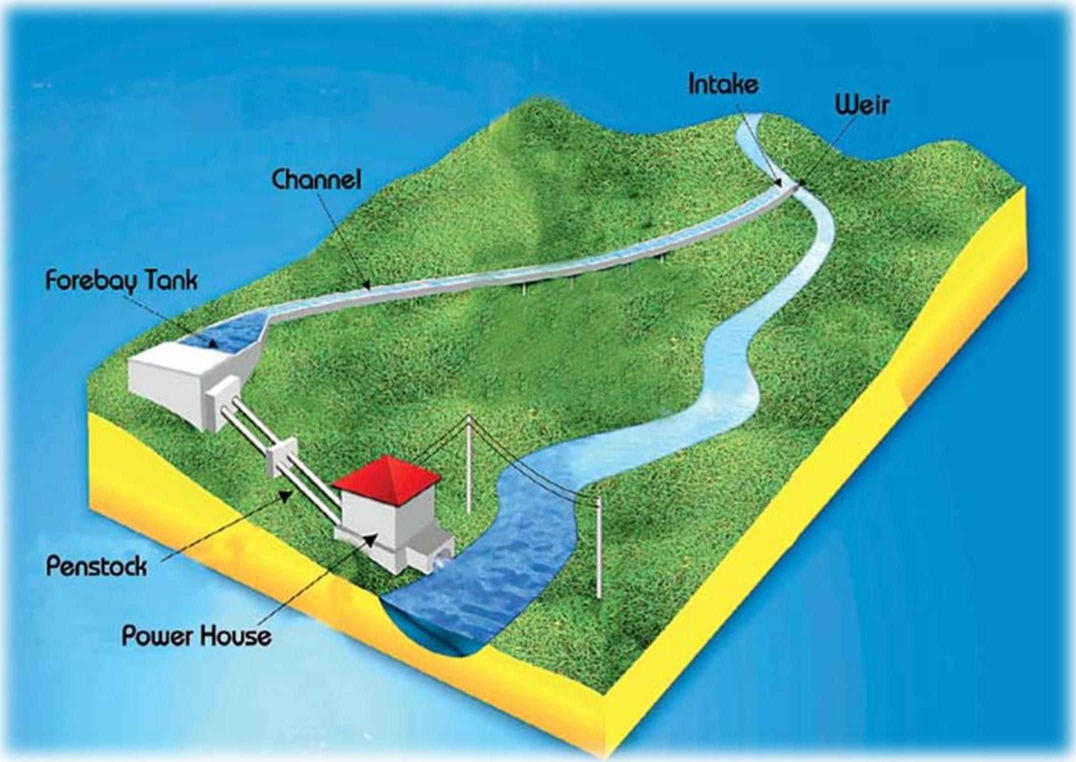

Figure 3: layout of typical mini hydro power plant

1.1.1 Weir, intake canal and penstock pipe line

In order to divert river flow from its natural path, a small barrier (weir) was built to raise the water level slightly on the upstream side. This allows water to pool behind the weir while allowing water to flow steadily over top of the weir. A bottom permeant opening is also kept to maintain steady flow alone rivers natural path which helps to maintain the downstream ecosystem. An intake mouth with an intake gate and trash rake is built at a side of the weir connecting to the intake canal. This trash rake blocks larges debris such as logs, tree branches that are floating along the river entering to the intake canal. The intake canal usually runs along the same contour line until it reaches to a rapid slope where the forebay tank is built.

A forebay tank is a basin-like structure where water is temporarily stored before going into penstock pipes. The storage of water in the forebay reduced its speed rapidly which allows silt and mud particles to be deposited at the bottom. This area is also known as the desilting tank usually constructed with a bottom flush outlet which will use to flush out the deposited silt particles in specific intervals. Another trash rake is normally located just before the penstock pipes to avoid entering of mid-size debris such as sticks, leaves to the turbine.

Penstocks are closed pipes that carry water down from the forebay to the turbines inside the powerhouse. Generally, they are made of steel, and water under high pressure flows through the penstock. these pipes are designed to resist the water hammer effect due to sudden closings during load rejections. (Generator disconnected from the grid) and a surge pipe is provided to mitigate the water hammer. Here, the potential energy is converted into pressure energy. There is also a loss of energy and it is related to the friction in pipes which, in turn, depends on the pipe diameter, the flow velocity, the surface roughness of the penstock, number of bends and it increases proportionally to the length of the Pipeline. Figure 4 shows the weir, intake canal, forebay, and penstock of a mini hydropower plant in Sri Lanka.

Figure 4: weir, intake canal, forebay and penstock of "Moragaha Oya" mini hydro power plant

1.1.2 Power house and electro mechanical equipment

Powerhouse is a building provided to shelter the hydraulic and electrical equipment. Generally, the whole equipment is supported by the foundation or substructure laid for the powerhouse. some machines like draft tubes, spiral casing, etc. are fixed within the foundation while laying it. A tailrace is constructed to discharge the outward flow of water from turbines to the river stream.

Hydraulic turbines coupled with electrical generators spin to convert the hydraulic energy into mechanical energy which is again converted into electrical energy and subsequently carries away from the power plant. A hydraulic or electrical governor system controls the intake flow of the turbines while controlling speed and electrical power output accordingly. A main intake valve is used to shut off the flow completely during an emergency shutdown.

The electrical system starts from the generator terminals. Current flows through a synchronous circuit breaker which is used in grid synchronization and protection tripping. Protection and control system helps to preforms the startups, grid synchronization, normal run, shutdown, and emergency shutdown operations. Most of the present mini hydropower plants are equipped with PLC or embedded computer-based control systems with digital protection relays and SCADA, HMI interfaces. A power transformer steps up the generated voltage to transmission line voltage level and an MV circuit breaker and switch gears are also included in this system. Figure 5 shows the electromechanical equipment of a mini hydropower plant.

Figure 5: Electrotechnical equipment of Moragahaoya mini hydro power plant

1.2 Multiple turbine operation

Generally, hydraulic turbines are of two types namely impulsive turbine and reaction turbine Impulse turbine is also called velocity turbine. Pelton wheel turbine is an example of an impulse turbine. A reaction turbine is also called a pressure turbine. Kaplan turbine and Francis turbine come under this category. Depending on the available flow and available water head, the type of turbine to be used is selected during the design stage of the power plant.

All of the above-mentioned turbines share one common negative characteristic which is having very low efficiency when operating with a lower percentage of turbine full design flow. The change of efficiency of hydraulic turbines with intake flow is shown in figure 6. This became a major challenge in mini-hydropower plants where water streams proved highly dynamic flow with changing weather (catchment rain) and unavailability of large water storage.

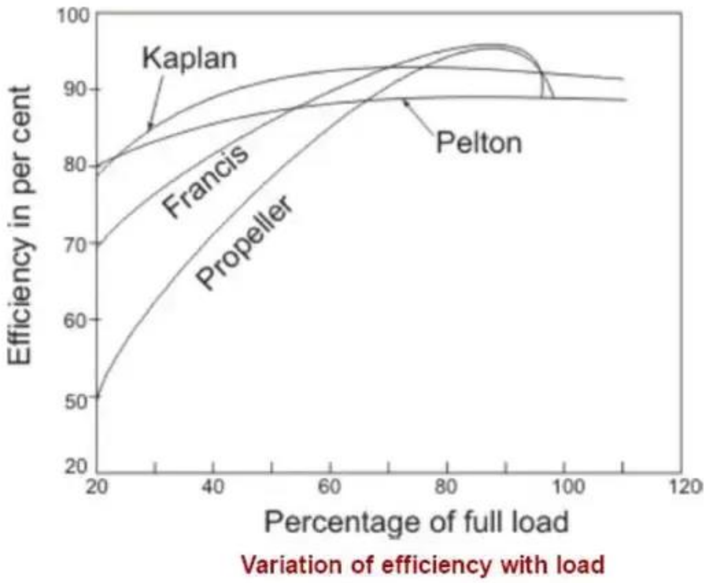

Figure 6: change of efficiency of hydraulic turbines with intake flow

To overcome this issue, designers have been including multiple turbines with different capacities in the power plan where the sum of flow capacities of turbines are equal to the design flow of the power plant. This way a power plant can operate its smaller capacity turbine in a higher percentage of turbine design flow rather than running a large-capacity turbine in a lower percentage of turbine design flow under the same available flow. This enables the power plant to operate in higher efficiency and thus maximize the power generation using available flow[18].

In order to distribute available stream flow between turbines, a flow distribution control technique is employed. Those controllers are designed to operate with or without human interaction depending upon the available technology.

1.3 Existing flow control techniques.

Mini hydropower plant control technologies have been evolved to a level where most power plants equipped with PLCs and embedded computers or at least digital PID controllers. Thus, advance digital control algorithms. Distribution of available water flow among turbines is one among many tasks handled by a power plant control system. In Francis turbines, flow intake to each turbine is physically controlled by opening and closing of wicket gates (guide vane). In Pelton wheel turbines same is achieved by moving the jet needle. There are two different flow distribution control techniques that can be found in present-day mini hydropower plants. Figure 7 shows the physical flow control mechanism in a Francis turbine.

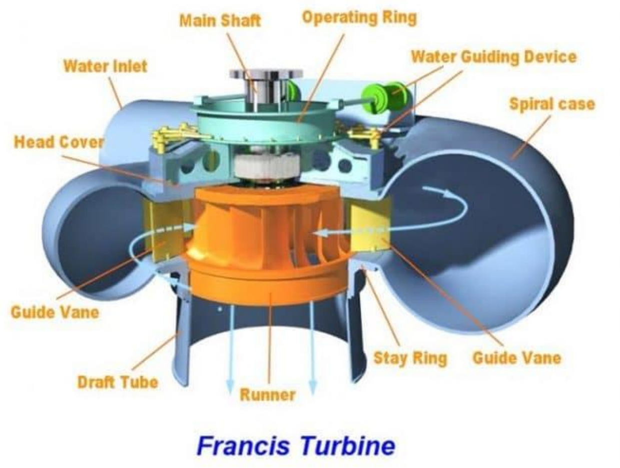

Figure 7 : physical flow control mechanism in a Francis turbine

1.3.1 Semi-automatic flow distribution control

In this method, one turbine is controlled using a closed PID loop. The controller's objective is to keep the forebay water level steady by controlling the wicket gate opening and sending water to the turbine balancing in and outflow of the forebay. This control strategy works until the controlled turbine reached its limits where fully open or fully closed position. When it happens, the forebay water level starts to rise and spill or vice versa. Subsequently, an operator has to intervene and adjust the second turbine's flow manually in a way that the controlled turbine comes back to half opening (refer to figure 8). In normal practice, the small turbine will keep as a controlled turbine to achieve maximum efficiency from the combined operation.

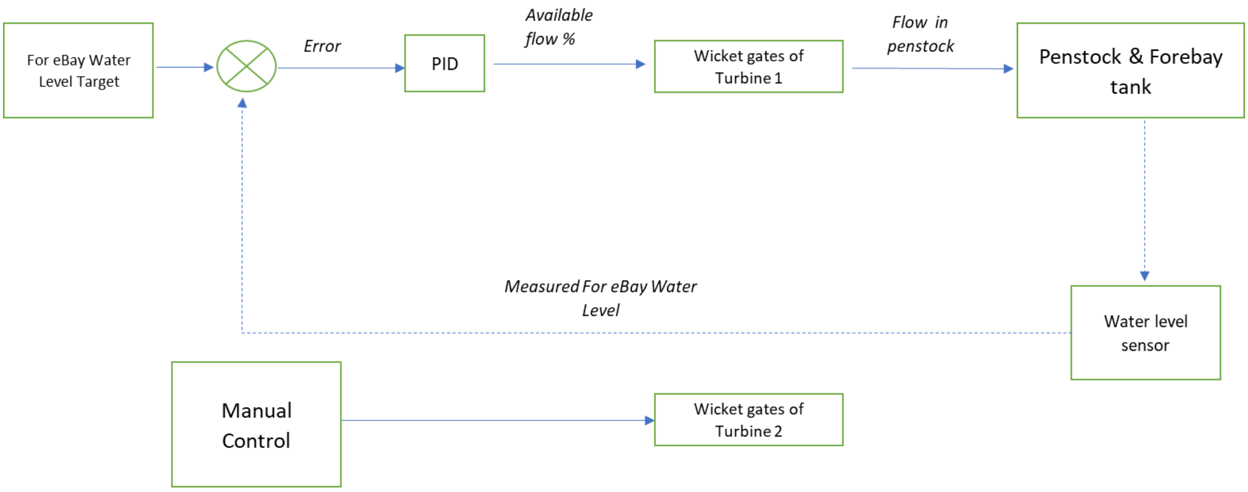

Figure 8: control block diagram of "Semi-automatic" flow distribution controller

1.3.2 Full-automatic flow distribution control

To overcome the drawbacks of the previous method, this method is implemented in most modern mini hydropower plants. But it required a digital controller such as a PLC are an embedded computer to implement this method. Unlike in the previous case, this method does not require human interference. A closed-loop PID controller will decide the amount of flow that can draw into the power plant while keeping a steady forebay water level. The PID controller output is then directed to a fixed flow distribution table which will decide the amount of flow that shall be allocated to each turbine. According to the distributed flow fractions, the controller will send control signals to each turbine's wicket gate actuators to maintain the level of opening. If any turbine reaches to fully closed state, an automatic shutdown sequence kicks in to shut down the turbines. (refer to figure 9) if it requires to start a deactivated turbine, an automatic startup sequence will take care of the activities up to grid synchronization. tuning of the flow distribution table is taken place during the commissioning stage and minor adjustments are made during continued operation.

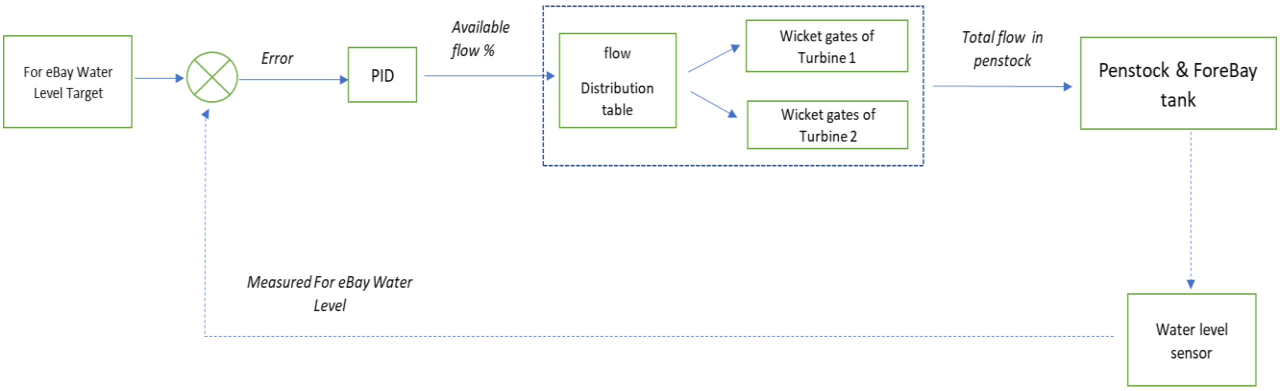

Figure 9: control block diagram of "full-automatic" flow distribution controller

1.4 Problem statement

Normally in a mini-hydro power plant, tuning of PID loop and flow distribution table is taken place during the commissioning period of the power plant. A Theoretical calculation has been done using penstock friction losses and turbine efficiency carves which are supplied by the manufacturer to determine expected powerplant output at each flow combination. Thereafter that data feeds to the flow distribution table. During the operation, the control software selects the best operating point for the available river flow at the moment and controls the wicket gates accordingly.

Table 1 shows the theoretically calculated output values of the "Moragaha Oya" mini hydropower plant. According to the calculations, the best operating flow combinations are highlighted in blue color where maximum output can be achieved during different available flows. As an example, when the available river flow is 0.45m3/s, the possible operating combinations can be found along the red line. The highest output is 271.72kW at 50% flow of turbine 1 and 0% flow of turbine 2.

Table 1: theoretically calculated flow distribution table of "Moragaha Oya" mini hydro power pant

	Unit 2 Flow										
Unit 1 Flow	0.00%	10.00%	20.00%	30.00%	40.00%	50.00%	60.00%	70.00%	80.00%	90.00%	100.00%
0.00%	0.00	72.02	143.91	215.49	310.10	420.68	516.38	620.41	722.68	809.89	873.99
10.00%	46.30	118.26	189.96	261.31	355.56	465.71	560.84	663.98	765.07	851.62	914.77
20.00%	92.57	164.39	235.92	306.92	400.64	510.15	604.56	706.82	807.56	892.75	955.41
30.00%	138.77	210.39	281.61	352.28	445.50	554.34	648.24	749.37	848.76	933.24	994.32
40.00%	199.92	271.27	342.11	412.31	505.05	612.94	705.71	806.41	904.26	987.50	1047.35
50.00%	271.72	342.70	413.07	482.68	574.51	681.62	773.37	872.51	969.92	1051.26	1110.42
60.00%	334.23	404.79	474.63	543.62	634.65	740.78	831.48	929.41	1024.95	1105.40	1162.46
70.00%	402.44	472.48	541.87	609.98	700.10	805.14	894.67	991.80	1085.33	1164.24	1219.77
80.00%	470.12	539.57	608.10	675.57	764.71	868.56	956.84	1052.00	1145.25	1221.82	1275.76
90.00%	528.80	597.61	665.41	732.06	820.18	922.83	1009.83	1103.55	1194.50	1270.19	1322.53
100.00%	572.78	640.96	708.04	773.87	860.99	962.45	1048.21	1140.53	1229.96	1304.10	1354.94
	Total power output (kW)										

1.4 m^3/s

0.9m^3/s

2.3m^3/s

During the operations of the power plant due to its runoff river construction, river water is directly entered into the intake canal as it flows in the river with floating debris and suspended particles. In conventional large-scale power plants, such objects get deposited as the flow reaches near-zero velocity at its large storage reservoir. But with the unavailability of such effective settling space, water only flows through trash rake and desilting tank in mini hydropower plants. As a result of this ineffective filtration, after short and intense catchment rain, a higher amount of mud, sand, and other floating particles are entered into the penstock pipe and then into turbines. If one tries to reduce the gaps of the trash rake to increase its effectiveness, rapid accumulation of debris like tree leaves will block the trash rake instantaneously resulting in a sudden shutdown of the power plant or even distortion of penstocks pipes due to air suctions in the worst-case scenario[17].

Even though the design calculations have been done assuming ideal water conditions (density, frictional coefficients), As a result of the above-mentioned contaminated water, Turbines are subjected to a small (but considerable) amount of power loss during continuous operations.

This gets worst when there is catchment rain and subsequent muddy water enters the turbine. Apart from that, the pre-tuned best operating points are not valid anymore with said changing water conditions. Therefore, power plant operators have to manually seek through the entire flow combinations to find the best operating points when water condition changes. After a while, a skilled operator may learn how to dispatch each turbine depending on the river water condition. But it does not fulfill the whole concept of "fully automatic flow distribution control". Thus, there may be instances the power plant operates in lesser capacity than available potential, especially during the night when operators are not on full alert.

Table 2 and table 3 shows such two instances (muddy water and clear water) of the "Moragaha Oya" mini hydropower plant where total output power reduced from its design values and the best operating points are not lies according to the theoretically calculated flow distribution table. The best operation point at 100% river flow is highlighted in yellow in both tables. Figure 10 also represents the same in as a 3D surface representation.

Table 2: flow distribution table of "Moragaha Oya" mini hydro power plant obtained during clear water situation

Turbines cannot operate in this region due to vibrations

Unit 1 Flow	Unit 2 Flow: 0.00%	10.00%	20.00%	30.00%	40.00%	50.00%	60.00%	70.00%	80.00%	90.00%	100.00%
0.00%	0.00	0.00	0.00	158.00	270.00	375.00	463.00	560.00	654.00	737.00	803.00
10.00%	0.00	0.00	0.00	158.00	270.00	375.00	463.00	560.00	654.00	737.00	803.00
20.00%	0.00	0.00	0.00	158.00	270.00	375.00	463.00	560.00	654.00	737.00	803.00
30.00%	130.00	130.00	130.00	322.28	405.50	514.34	599.24	690.37	786.76	857.24	922.00
40.00%	188.00	188.00	188.00	388.31	474.05	574.94	660.71	752.41	848.26	916.50	971.00
50.00%	258.00	258.00	258.00	458.68	544.51	646.62	732.37	821.51	918.92	986.26	1030.00
60.00%	322.00	322.00	322.00	521.62	607.65	712.78	798.48	884.41	976.95	1036.40	1073.00
70.00%	388.00	388.00	388.00	591.98	680.10	776.14	854.67	950.80	1035.33	1103.24	1128.00
80.00%	455.00	455.00	455.00	658.57	739.71	835.56	916.84	1008.00	1094.25	1165.82	1180.00
90.00%	512.00	512.00	512.00	714.06	798.18	891.83	975.83	1067.55	1156.50	1230.00	1213.00
100.00%	554.00	554.00	554.00	760.00	841.00	941.00	1010.00	1100.00	1194.00	1210.00	1190.00

Total power output (kW)

Table 3: flow distribution table of "Moragaha Oya" mini hydro power plant obtained during mudy water situation

Turbines cannot operate in this region due to vibrations

Unit 1 Flow	Unit 2 Flow: 0.00%	10.00%	20.00%	30.00%	40.00%	50.00%	60.00%	70.00%	80.00%	90.00%	100.00%
0.00%	0.00	0.00	0.00	157.47	267.35	373.32	454.08	559.85	650.87	728.64	800.82
10.00%	0.00	0.00	0.00	157.47	267.35	373.32	454.08	559.85	650.87	728.64	800.82
20.00%	0.00	0.00	0.00	157.47	267.35	373.32	454.08	559.85	650.87	728.64	800.82
30.00%	124.39	124.39	124.39	314.78	404.03	512.53	598.80	689.11	779.66	856.33	917.49
40.00%	186.63	186.63	186.63	379.12	467.82	567.06	656.47	746.48	840.73	915.60	966.55
50.00%	250.69	250.69	250.69	457.99	534.77	642.77	726.46	813.87	912.32	980.94	1029.64
60.00%	319.01	319.01	319.01	515.20	606.66	706.31	797.79	876.73	974.56	1031.98	1069.97
70.00%	383.32	383.32	383.32	588.96	678.16	772.38	854.20	945.97	1026.73	1095.29	1127.27
80.00%	450.00	450.00	450.00	648.58	735.13	835.35	910.26	1006.51	1093.68	1165.24	1170.98
90.00%	510.00	510.00	510.00	708.88	794.77	884.75	973.84	1062.27	1154.15	1181.41	1207.76
100.00%	550.00	550.00	550.00	753.21	834.85	940.02	1002.73	1098.56	1190.63	1200.42	1188.04

Total power output (kW)

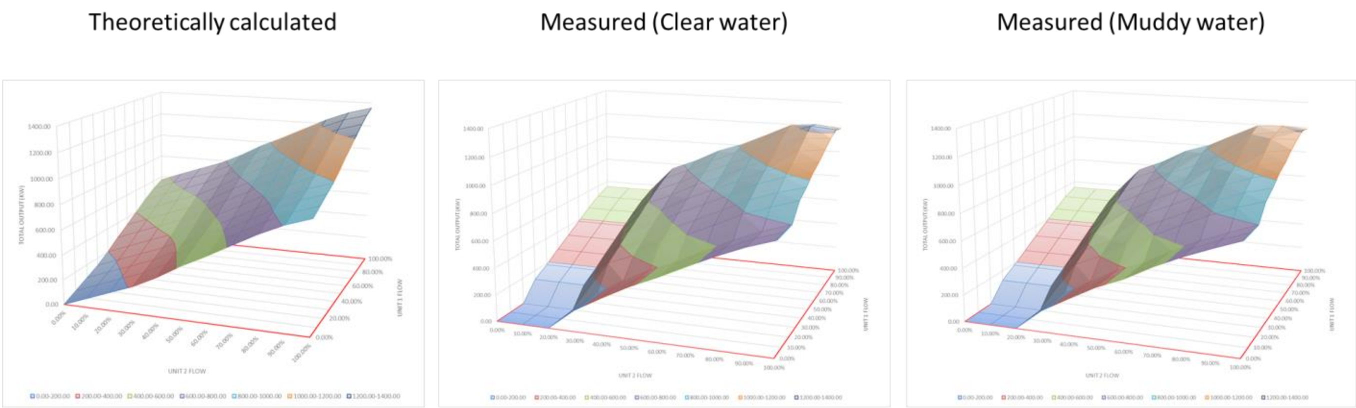

Figure 10: Total power output variation of “Moragaha Oya” mini hydro power plant (theoretical and two actual instances)

To address this problem, there must be a system that can update flow distribution table values frequently by assessing water conditions.

Having considered that this research aims to identify the relationship between water quality parameters and power loss and develop an intelligent controller capable of distributing water flow between turbines based on identified inputs which ensure maximum power generation at an available flow

1.5 Study source (“Moragaha oya” mini hydro power plant)

“Moragaha Oya” mini hydropower plant is located in the Kandy district of Sri Lanka. The power plant has been developed and is being operated by “Resus Energy PLC” which is a Sri Lankan IPP company. “Moraha Oya” is a tributary of the “Hulu Ganga” river that eventually merges into “Mahaweli” river which is one of the major rivers in Sri Lanka. This power plant is equipped with two Francis turbines and synchronous generator sets built by Gugler water turbines – Austria and Marelli Motori Group – Italy. The control system built by Wassi Systems – Belgium consists of a fully automatic flow distribution controller implemented on an embedded PC.

This power plant is an ideal source to study the subject problem because this power plant consists of a small catchment under the effect of dynamic weather conditions in the “Knuckles” Mountain range and a longer penstock pipe system with a number of bends which are key factors contributes to the discussed power reduction. Also, the flexible control system enables easy software modifications and hardware integrations. The important data of the power plant mentioned below

- Type : Grid connected , embedded generator (no dispatch control)
- Location : Huluganga , Kandy
- Capacity : 1500 kW

- Turbines : 2 Nos (960 kW , 616 kW) vertical Francis with hydraulic governors
- Head : 74.88 m
- Design flow : 2.3 m^3/s
- Penstock length : 1.3 km
- Catchment size : 20.5 km^2
- Flow distribution control : Fully automatic using an embedded computer

1.6 Methodology

1. *Collect data of the power loss in "Moragahaoya" mini hydro power plant.*
2. *Literature review.*
3. *Identify the possible relationships between water quality parameters and power reduction.*
4. *Preform experiments to validate the identified relationships.*
5. *Identify the most suitable artificial neural network (ANN) structure for the size of available data set*
6. *Develop a software tool including Artificial neural network and linear approximation to generate 2^{nd} degree surface.*
7. *Develop a software tool to collect data from external sensors connected to power plant control computer*
8. *Develop a GUI by integrating all software components which facilitates training data collection, training of the ANN and update of flow distribution table (Intelligent controller).*
9. *Design, develop and install additional hardware (sensor integration) to measure turbidity and wicket gate openings.*
10. *Training data collection during normal operation of the power plant and train the ANN.*
11. *Enable the intelligent controller to update the flow distribution table and collect power generation data to validate the performances of the controller.*

2. LITERATURE REVIEW

A proper literature review is very important for identifying the specified scope of the research, collecting previous and ongoing findings related to the research. This is very critical to avoid repeat work.

The power output of a typical hydraulic turbine is given by the following equation

$$P= Q \times (h_t - h_f) \times \rho \times g \times \eta$$

Where P = mechanical power output, Q = input flow rate, ht = total available head, hf = frictional head loss (function of Q), ρ= density of the water, g = gravitational acceleration, and "η"= efficiency of the turbine (function of Q). Among these parameters both water density (ρ) and frictional head loss (hf) have been identified as the parameters affected by water quality variations.

Apart from that, a proper literature review must be carried out on selecting the most suitable artificial intelligence (AN) technique to achieve the stated objectives. Since this study consists of a large number of past data and analyses of their relationships, ANN has been identified as the AN tool for this study. A proper ANN structure suits with available data need to be selected.

Accordingly, the following areas were reviewed.

1. Impact of floating derbies to the frictional head loss in penstock pipes.
2. Variation of river water density with the changes of water quality and reasons for the water quality variations
3. Methods of selecting most suitable ANN structure for given data set.
4. Existing uses of ANN in mini hydro power plants

2.1 Effects to the Hazen – William’s coefficient by floating debris

When calculating the frictional losses in penstock pipes, Hazen- William’s equation is used. This empirical consists of Hazen – William’s coefficient which is an experimental value obtained based on the inner surface condition of the used pipes. In most design calculations, pre-obtained Hazen – William’s coefficients are used from pipe datasheets. This reference questioned the consistency of the friction losses in a pipe and thus the validity of Hazen – William’s equation in design calculations. Hazen – William’s equation is given below

$$h_f = \frac{10.67 L Q^{1.852}}{C^{1.852} d^{4.87}}$$

Where, h_f = frictional head loss, C= Hazen Williams constant, Q=flow rate (discharge), L= length of pipeline and d = diameter of the pipeline.

According to Chyr Pyng Liou [1], change of flow Reynolds number due to the collision of floating debris of the water and changes of the internal surface of the pipe due to aging leads to make significant changes and inconsistency of the frictional loss in a given pipe.

2.2 Reduction of potential energy of water flow due to silt

Alan V. Jopling, Donald L. Forbes [2] discuss the significance of silt content to the reduction of the potential energy of a water flow. The authors have conducted an experiment using a flume and silted water. The study was to measure the parameters such as silt deposited, Raynolds number, and stream potential energy.

The results of their study show a significant reduction of stream head with the incensed silt density. Also, this

indicates the further reduction of the stream head with slit depositions and increment of Reynolds number. This again leads to further reductions of stream head due to bottom and sideways friction loss.

2.3 Variation of water density due to micro particles.

A. Wüest, G. Piepke, and J.D. Halfman [3] had conducted a study to identify the relationship between water quality indications such as total dissolved solids (TDS) and total suspended solids (TSS). Both TDS and TSS are measurable indications that are used to determine the number of micro partials of water. According to the definitions the micro partials which are having a mean radial less than 2µm can be categorized as dissolved particles and the micro partials which are having a mean radial greater than 2µm can be categorized as suspended particles.

this research shows the domination of the relationship of microparticle presence to density stratification of lake water than the same relationship with the temperature variation. It also suggests that dissolved gases such as CO2, CH4, and H2S are also contributing significantly to the density stratification.

Turbidity current is an underwater phenomenon that occurs due to the density changes of the water caused to be high contaminations. In this paper, the author focused on the density changes of the water due to the presence of foreign particles.

Gerard V. Middleton [4] has conducted an experiment using artificial suspended particles and water to study the behavior of turbidity currents. By looking at the results it is visible that there is a negative effect on the water density due to suspended particles and subsequent formation of upward turbidity currents.

2.4 Relationship between catchment characteristics and debris content of river water

Identification of the catchment characteristics which contribute to the presence of micro partials in stream water is vital to this research. Sunita Singh and Arabinda Mishra [5] have clearly identified the main

governing catchment parameters for the microparticle presence. As pre the research, forest cover, terrain condition, and rainfall intensity are contributing to increasing the level of water turbidity and thus increasing the TDS and TSS values. This study indicates that reduction of 1% forest covers results increment of 8.41% turbidity and 4.17% TSS.

the research also shows the intensity of rainfall increase the water turbidity even the total annual rainfall remains low. The elevation characteristic of the catchment also contributes to the reduction of the water quality by increasing soil erosion and thus increasing the TDS of the water. The research also shows that the frequency of water quality changes depends on the size of the catchment and rainfall patterns.

2.5 Applicability of ANN technique to this specific problem

Jure Zupan [6] provides a clear introduction to ANN and suggests the possibility of using the ANN technique in this particular exercise. ANN technique is suitable for a system with input and output domains and the dependence of input to the output might nonlinear. Solving such a system and predicting outputs based on given inputs is an objective of this research and the system is identified as a "Black Box" (refer to figure 11).

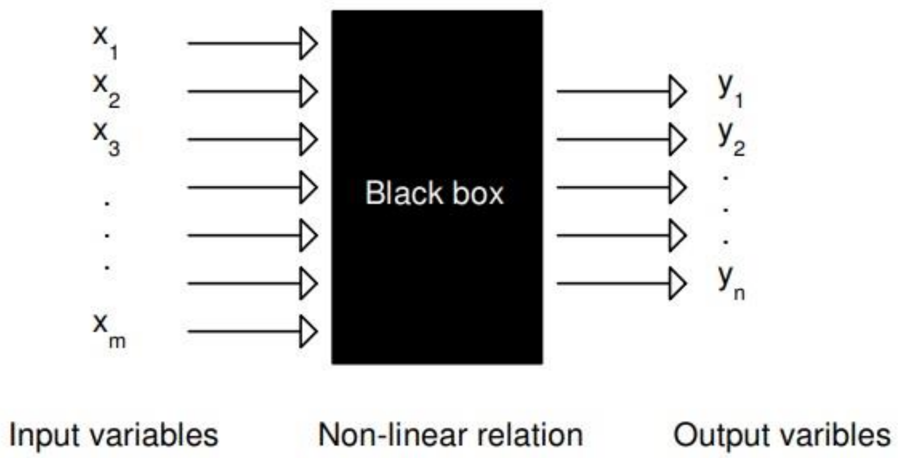

Figure 11: A typical "Black Box" system which can be solve by using ANN

The ANN is supposed to mimic the action of an actual neuron system. It accepts signals from outside sensors or neighboring neurons (xi) and processes the signal in a pre-defined simple way[15] . Then it releases an output signal to the outside environment (yj) or another neighboring neuron. This whole action is mathematically modeled in an ANN and such a model is shown in figure 12.

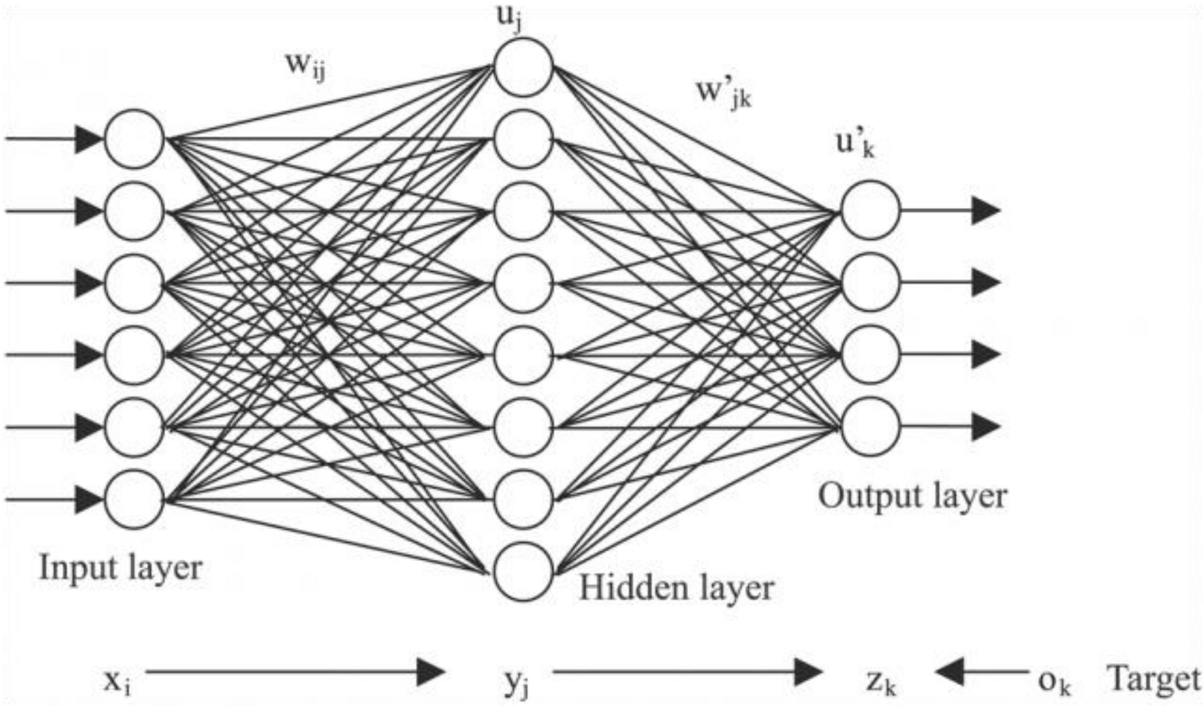

Figure 12: An ANN model

The results of all inputs in a given neuron are multiplied with weight coefficient (wji) which is similar to the strength of each outside signal captured by a biological body. Then the results are added up and the output will be obtained using a transfer function.

Here the transfer function represents the "knowledge" that a biological body obtained by constant adaption of synapses to different input signals causing better and better output signals. As per this reference most cases of the ANN approach the networks of neurons are composed of neurons having the transfer function of a sigmoidal shape. The mathematical equations which provide output according to inputs are shown below

$$u_j = \sum_{j=1}^{m} w_{ij} x_i$$

$$y_j = \frac{1}{(1 + e^{-u_j})}$$

Since this particular problem consists known set of outputs for specific inputs at hand according to the author, this requires a supervised training approach. Such a supervised training approach is mentioned in this reference namely Error Back-Propagation. During the training, available data have to divide into three sets where the first one is the training set, the second the control (or fine-tuning set) and the third one is the final test set. Suppose if the untrained ANN output for given input xi is yi and the desired output is ti according to the data in hand. Then the error δi is calculated and the weights of the output layer are corrected. And the same process is repeated to the next inner layer and so on. The correction process is expressed in the below equations and the parameters η and μ are called learning rate and momentum and are mainly between 0.1 and 0.9 [15] .

$$\delta_i = y_i - t_i$$

$$\Delta w_{ji} = \eta \delta_j y_i + \mu \Delta w_{ji}\ (Previous)$$

Once training is completed, the performance of the trained ANN is evaluated using a previously segregated test data set. The root mean square (RMS) error is such performance indicator calculated as follows where tsi and ysi are outputs related to input xsi which ysi network output and tsi is related sth test data in hand.

$$\text{RMS error} = \sqrt{\frac{\sum_{s=1}^{r}\sum_{i=1}^{n}(t_{si} - y_{si})^2}{rn}}$$

2.6 Optimization of ANN structure based on the nature of given data

To decide the best suits ANN structure, findings of Khaled M. Matrouk, Haitham A. Alasha'ary, Abdullah I. Al-Hasanat, Ziad A. Al-Qadi, and Hasan M. Al-Shalabi [7] is referred to. In this reference, the authors have performed a number of experiments for the same data set using different ANN structures. Mainly they have used various combinations of hidden layers and learning rates and thus they have tried to obtain relationships of ANN parameters that provide the best performances for a given data set. The result of such experiment is shown in table 4 and table 5.

Table 4 : ANN simulation Data- Absolute error for zero hidden layer

Number of hidden layers (x1)	**Epochs (x2)**	**Learning rate (x3)**	**Training time In msec (TT)**	**Absolute error % (AT)**
0	5	0.1	82	26.8
0	10	0.1	72	29.9
0	20	0.1	122	1.4
0	30	0.1	135	5.4
0	40	0.1	87	30
0	50	0.1	224	2.2
0	60	0.1	276	0.5
0	100	0.1	295	0.9

Table 5 : ANN simulation Data- Absolute error for one hidden layer

Number of hidden layers (x1)	**Epochs (x2)**	**Learning rate (x3)**	**Training time In msec (TT)**	**Absolute error % (AT)**
1	5	0.1	63	26.8
1	10	0.1	86	29.9
1	20	0.1	83	1.4
1	30	0.1	157	5.4
1	40	0.1	159	30
1	50	0.1	159	2.2
1	60	0.1	221	0.5
1	100	0.1	323	0.9

As per the above data, it is obvious that the absolute error is decreasing with the increment of hidden layers. But at the same time, the computation time will also increase. This can't be considered as a possible issue for the subject problem since training time does not relate to the actual operation of the proposed intelligent controller. the variation of the absolute error for different numbers of hidden layers has been obtained and is shown in figure 13.

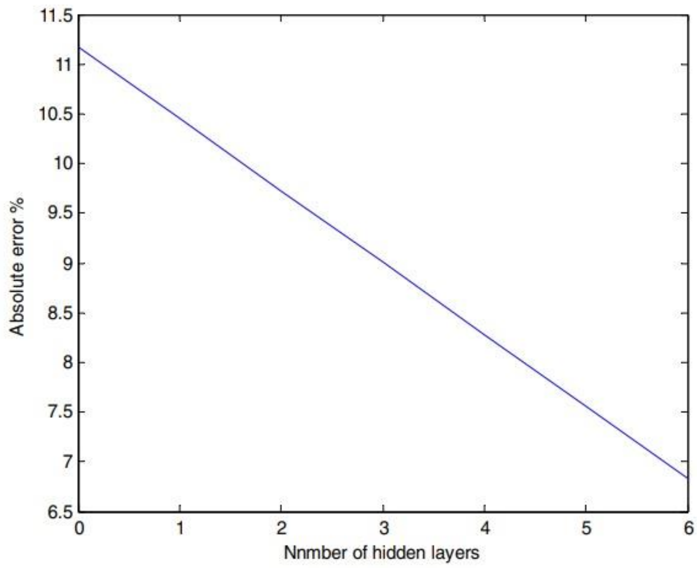

Figure 13: ANN simulation Data- variation of absolute error with number of hidden layers.

This reference is concluded with a linear relationship equation obtained by simulation data and the below equation shows the negative relationship of absolute error and number of hidden layers whare at= Absolute error, x1= number of hidden layers, x2 = number of epochs, and x3=learning rate.

$$at = 11.1747 - 0.7242x_1 + 0.0007x_2 - 14.4027x_3$$

2.7 Utilization of ANN technology in problems of similar caliber

It is vital to refer to similar research where ANN technology is utilized in mini hydropower plants, especially in Sri Lanka. In this research, the researchers are focused on predicting a mini hydropower plant output power using catchment rainfall data which feeds into an ANN. Anushka Perera, Upaka Rathnayake have published a paper [8] for a similar condition where the subjected catchments and streams share similar geographical and climate conditions. Even though this paper address a different problem state, the results give a significant indication that the Use of data such as rainfall via an ANN to predict data related to the power output of a mini-hydropower plant is successful. The following relationship function is used for the study where PowerDenawaka = monthly generated power of the "Denawaka Ganga" mini hydropower plant (GWh) and the RFi is the monthly cumulative rainfall (mm) of the "Denawaka" catchment.

$$\text{Power}_{\text{Denawaka}} = \emptyset(RF_i, RF_{i+1}, \dots \dots \dots RF_n)$$

A similar exercise has been conducted on the "Erathna" mini-hydropower plant but using an unsupervised learning technique because of the unavailability of the historical rainfall data of the "Erathna" catchment. The results of actual monthly power generation output Vs ANN estimation for "Denawaka Ganga" are shown below figure (figure 14). The RMS error is within the acceptable range and hence the validity of the supervised ANN model is confirmed. The performance of the ANN training is also shown below (figure 15).

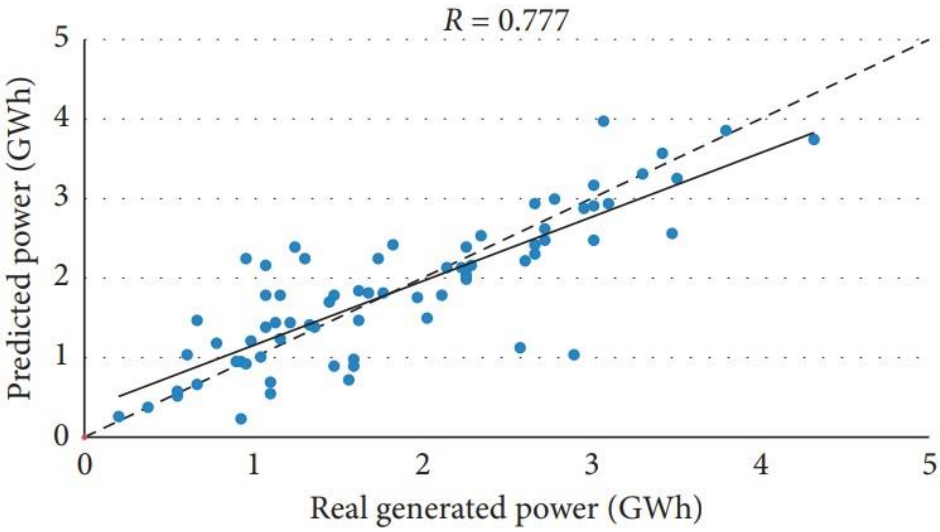

Figure 14: Actual and ANN predicted monthly power generation data of "Denawaka Ganga" mini hydro power plant

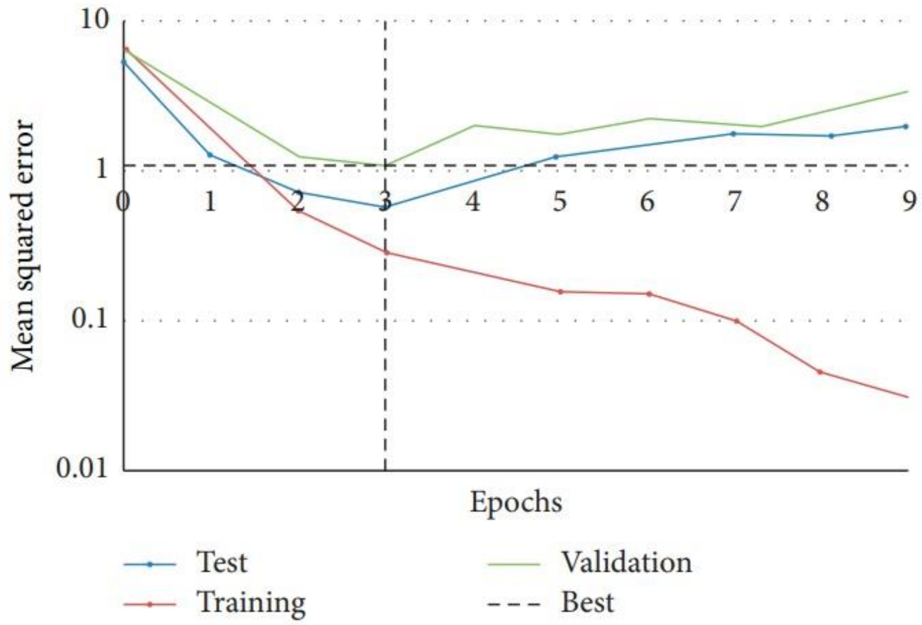

Figure 15: ANN training performances of “Denawaka Ganga” mini hydro power plant model

However, the authors have also concluded that the performances of the unsupervised ANN training model are not in an acceptable range. Hence the authors do not recommend the use of an unsupervised ANN tool to handle such data.

Also, Miyuru B. Gunathilake, Chamaka Karunanayake, Anura S. Gunathilake, Niranga Marasingha, Jayanga T. Samarasinghe, Isuru M. Bandara, and Upaka Rathnayake have taken predicted streamflow of tropical Sri Lankan catchments using two different methods[9]. Suitability of traditional hydrology modeling tool “HEC-HMS” and ANN model for Sri Lankan tropical catchment is compared in this study. The “Seethawaka Ganga” stream and its upper catchment of the “Maliboda” area are selected for this study. The target catchment is similar to the subjected “Moragahaoya” catchment in both geographical and weather conditionally. Both catchments are fed by all northeastern, southwest, and intermediate monsoons. Human activities such as cultivation and natural characteristics such as flora and fauna are also ideal in both cases. Same like “Hulu Ganga”, the “Seethawaka Ganga” is also utilized by a number of mini hydropower plants. The ANN predicted streamflow and actual streamflow are shown in the below figure (figure 15) and the comparisons of both ANN and HEC-HMS predicted flow discharge with actual flow discharge is also shown. (Figure 16)

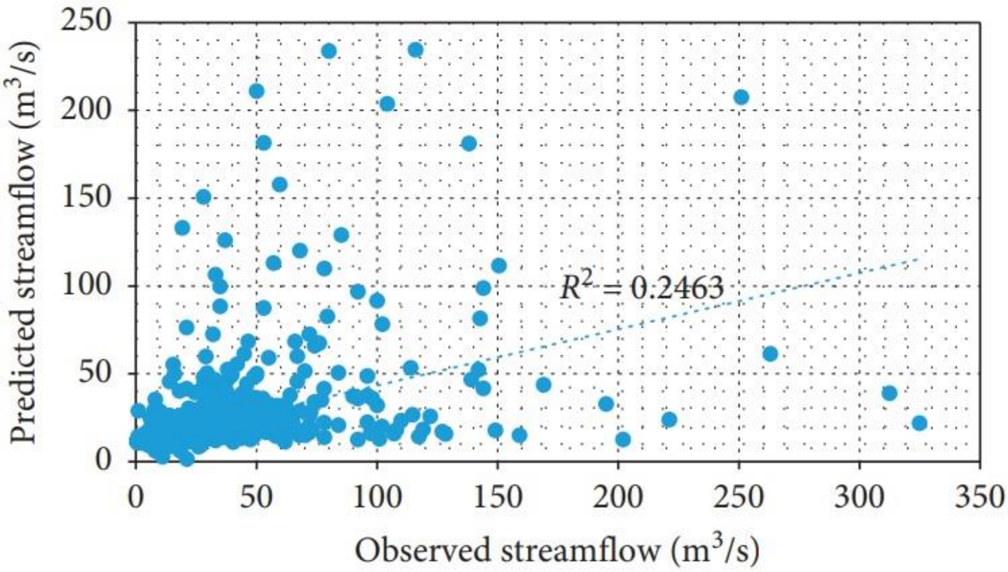

Figure 16 : Actual and ANN predicted stream flow of “Maliboda” Catchment

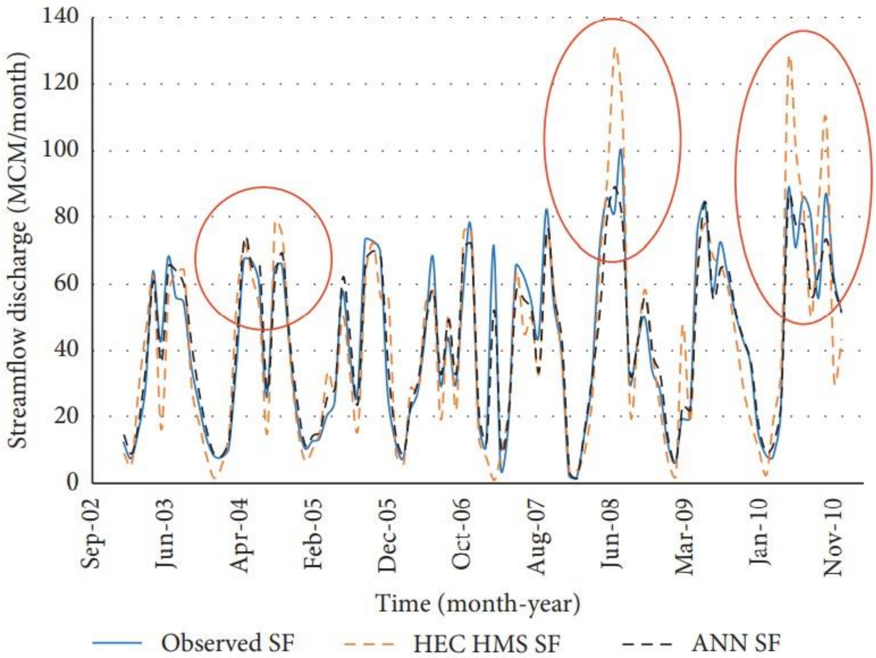

Figure 17: Monthly discharge of “Maliboda Catchment” – Actual data, ANN predicted data and HEC-HMS Predicted data

According to figure 16, the RMS error of the ANN predicted data is in an acceptable range, and as per figure 17, the ANN predictions are much more accurate than HEC-HMS. Hence this paper confirms the validity of usage of ANN for streamflow predictions in Sri Lankan small stream catchments.

3. DESIGN AND DEVELOPMENT OF INTELLIGENT CONTROLLER

3.1 Introduction

After a thorough literature review, the possible reasons for the output power loss and changes in the operating point have been identified. As per Chyr Pyng Liou [1], the large size floating derbies will change the internal friction loss of the penstock pipelines. And as Alan V. Jopling and Donald L. Forbes [2] argue, the amount of silt in the streamflow also impacts the friction losses in penstock pipelines. Also, the literature suggested the presence of organic and non-organic microparticles in the streamflow led to a variation of the water density [3],[4]. Apart from that Sunita Singh and Arabinda Mishra [6] shows the contribution of catchment rainfall and reduced forest cover to the increment of stream derbies content and microparticles.

But a separate study has to be carried out to identify accurate measurements to quantify the content of microparticles and floating debris in this particular catchment thus the identified measurements can be used as the inputs for the intelligent controller. therefore, a series of experiments have been carried out to seek the validity of the following relationships with stated measurements stated in table 6.

Table 6 : Stream measurements and the parameters intended to link

Measurement	**Strem parameter which intended to link with measurement**
Turbidity	Quantity of micro particles - TDS
Turbidity	Quantity of micro particles - TSS
6-hour catchment rainfall	Quantity of floating debris
12-hour catchment rainfall	Quantity of floating debris

The same turbidity sensor which supposed to use continually with the intelligent controller is used to get turbidity reding for the future convenience.

3.2 Relationship of turbidity and TDS

The total dissolved solids are defined as the number of microparticles present in the water of which the mean diameter of a particle is less than 2µm. To evaluate the TDS of a given sample, careful laboratory analysis has to be carried out. 12 water samples have been collected from the Moragaha Oya mini hydropower plant forebay tank at different water conditions and the turbidity sensor steady reading was also noted together with the samples. Even though the sensor is designed to work with nephelometric turbidity units (NTU), due to calibration difficulties the output is noted as a percentage of its total output voltage scale. Thereafter the samples were analyzed at “Mahaweli water quality laboratory” at Madatugama Sri Lanka as shown in figure 18.

Figure 18 : Laboratory testing of water samples to analyze micro partial content.

3.2.1 Methodology

The standard methodology for TDS analyzation is found in the references [10] is adopted and the performed procedure is described here. Initially, to measure total dissolved solids, a clean porcelain dish that has been washed and dried in a hot air oven at 180C for one hour is taken and weighed the empty evaporating dish in analytical balance. The sample is mixed well and poured into a funnel with filter paper and filtered approximately 80 -100 mL of sample. By this the particles of which mean radials is greater than 2μm are eliminated. Using a pipette,75mL of filtered sample is transferred into the porcelain dish. The oven is Switched on and allowed to reach 105°C. during the pre-heat. Oven and furnace temperatures are Checked and regulated frequently to maintain the desired temperature range. Thereafter the porcelain dish is Placed in the hot air oven and care was taken to prevent splattering of the sample during evaporation or boiling. The sample is dried until it gets to constant mass. The drying process took part for a long duration of up to 2 hours to eliminate the necessity of checking for constant mass frequently. Later the container is Cooled in a desiccator. this desiccator is designed to provide an environment of standard dryness and the dryness is maintained by the desiccant found inside. the lid was not kept off for prolonged periods which leads to the desiccant to be soon exhausted. the desiccator cover is kept greased with the recommended type of lubricant in order to seal the desiccator and prevent moisture from entering the desiccator as the test glassware cools. The dish was weighed again as soon as it has cooled down and it avoid the absorption of moisture due to its hygroscopic nature. The final weight is noted and the initial dish weight is subtracted from the final total weight. The answer is used to calculate the TDS in mg per liter. The procedure is shown in figure 19

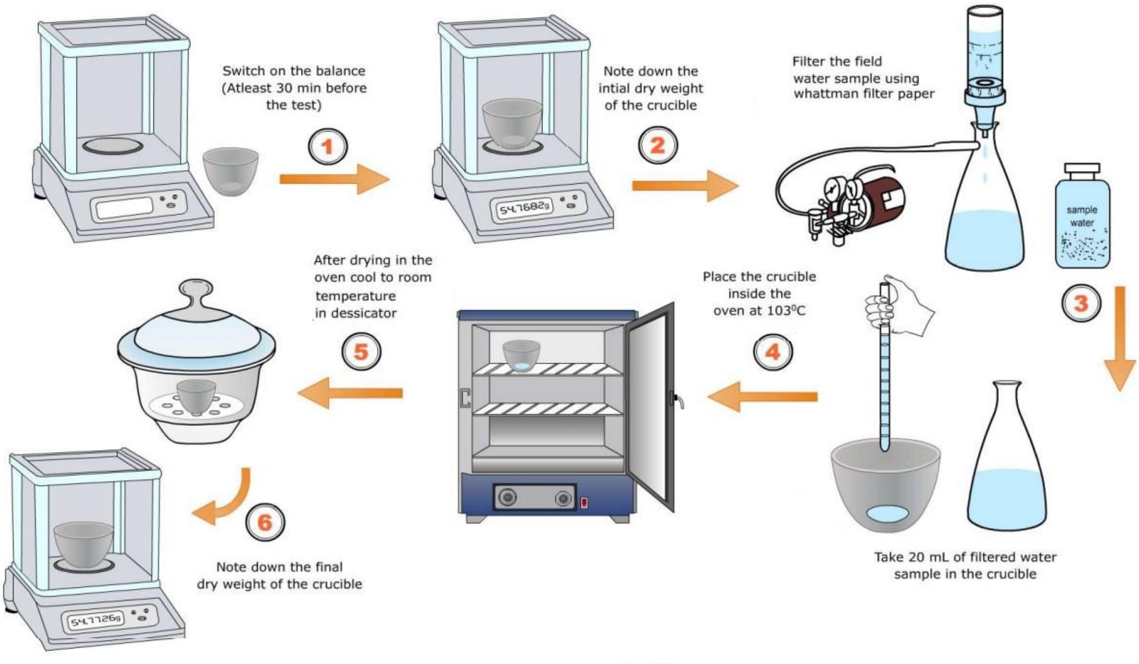

Figure 19 : Laboratory procedure for TDS analyzation.

3.2.2 Results

Each of the 12 samples were analyzed for the TDS and the obtained results ware compared with the related turbidity measurements. (Figure 20)

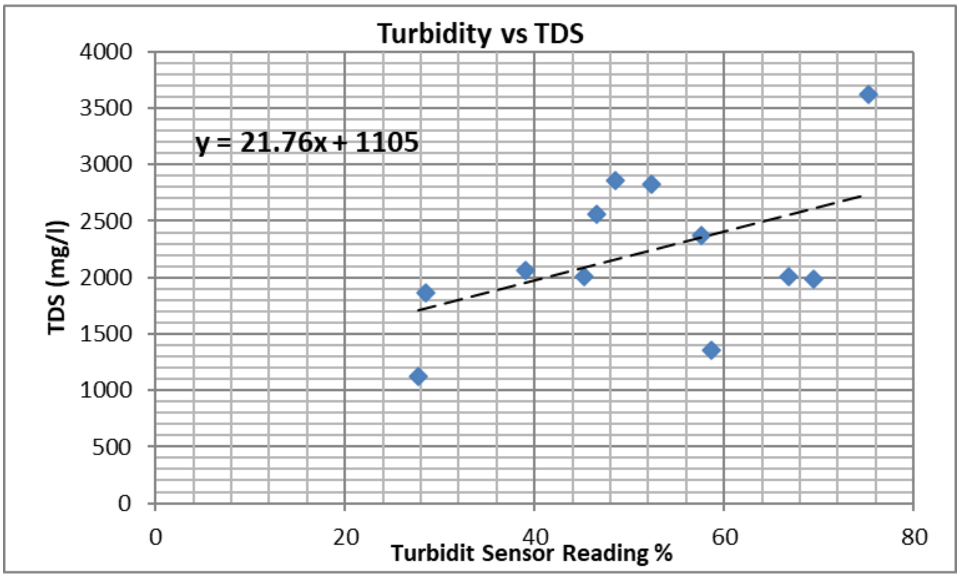

Figure 20 : Results – TDS and turbidity sensor readings

The results show a near-liner relationship, thus it is possible to argue that turbidity measurement can be used as a measure of TDS in the stream water of this particular case.

3.3 Relationship of turbidity and TSS

Total suspended solids (TSS) are defined as the microparticles of which the mean particle diameter of a particle is greater than 2µm. same as the TDS analysis. Another 12 samples were taken from the forebay of the Moragaha Oya mini hydropower plant and steady turbidity readings were also noted along with each sample. The same sensor arrangement is used to get the readings.

3.3.1 Methodology

The standard methodology for TSS analyzation is found in the references [10] is adopted and the performed procedure is described here. First, a filter paper is weighed and then Placed on the filtration apparatus in a filter flask. The sample has been mixed well and then poured into a graduated cylinder up to the volume of 75ml. suction is applied by suction pump to filter flask and the filter paper is seated with a small amount of distilled water. Previously selected sample volume is Poured into filtration apparatus. The suction action is to Draw the sample through a filter into a filter flask. Thereafter the graduated cylinder is Rinsed into filtration apparatus with three successive 10 mL portions of distilled water, allowing complete drainage between each rinsing and thus making sure that all the suspended partials drained into the filter paper. The suction pump is Continued for three minutes after filtration of the final rinse is completed. Finally, the filter paper is Dried in an oven at 103-105°C for about 1 hour, and the filter paper is kept in a desiccator to cool the filter to room temperature. When cooled, the weight of the filter paper is measured and the initial weight is subtracted from the answer. The result is used to calculate the TSS value in the sample in mg per liter. The analysis procedure is shown in figure 21.

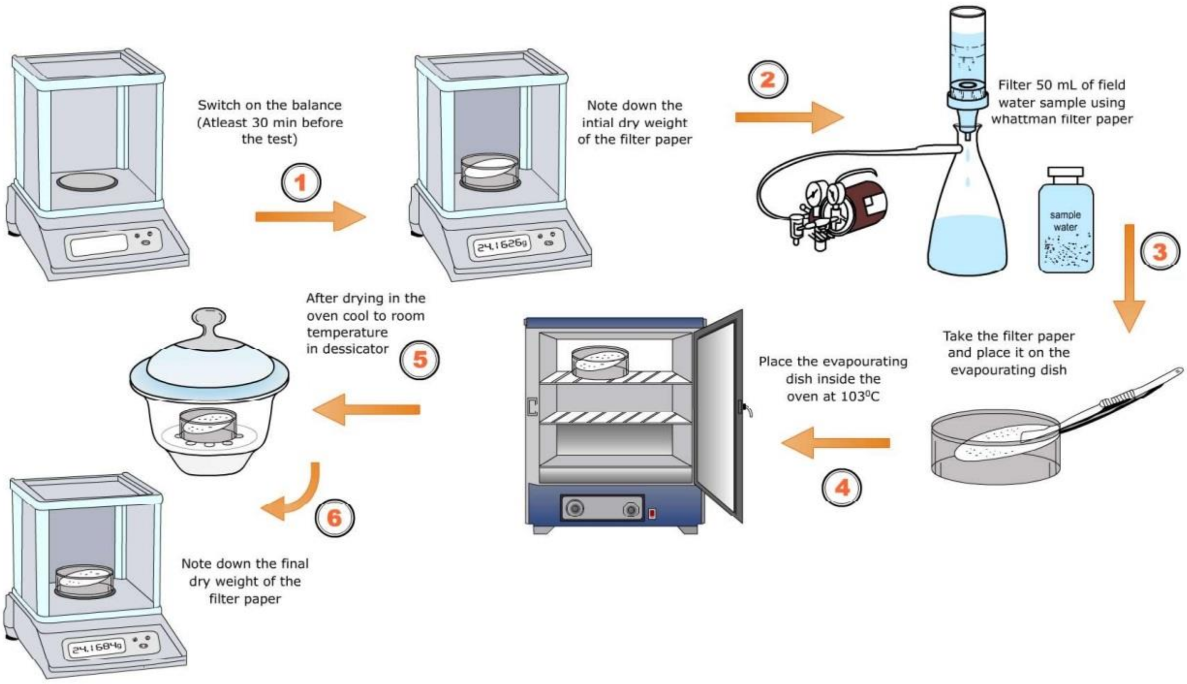

Figure 21 : Laboratory procedure for TDS analyzation.

3.3.2 Results

Each of the 12 samples was analyzed for the TSS and the obtained results were compared with the related turbidity measurements. (Figure 22)

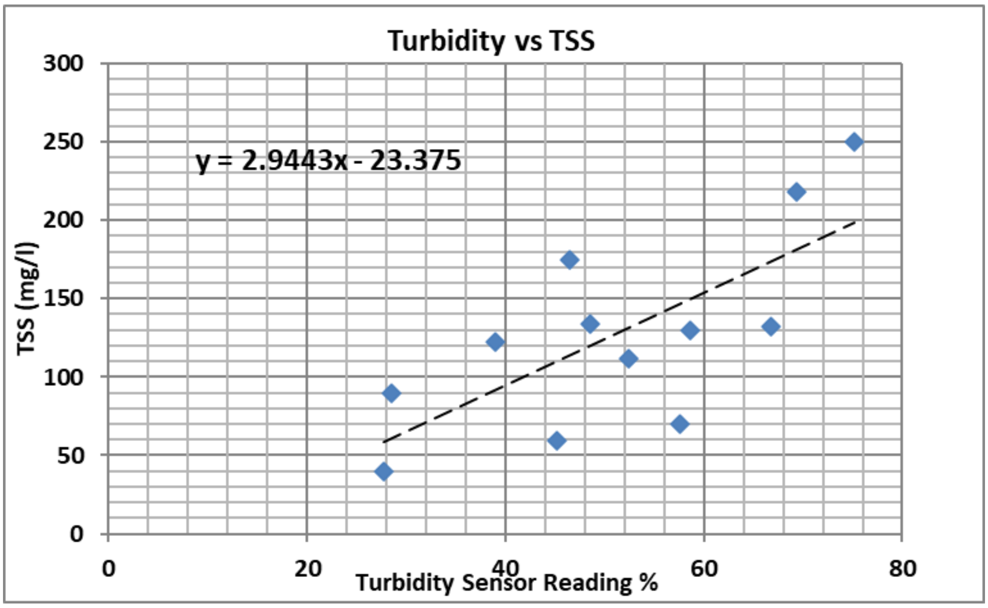

Figure 22 : Results – TSS and turbidity sensor readings

The results show a near-liner relationship as per figure 22, thus it is possible to argue that turbidity measurements can be used as a measure of TSS in the stream water of this particular case. Therefore, is decided to use turbidity sensor reading as one input to the ANN-based intelligent controller.

3.4 Relationship of floating derbies and rainfall

Since there is no specific measurement technique found in the literature to obtain the relationship between rainfall and floating debris, a straightforward method is used. Since the focus is limited to the floating debris which is supposed to enter the penstock and eventually to turbines causing problematic power loss, the debris sampling location must be lying after the trash rakes of the mini-hydro power plant.

3.4.1 Methodology

To ensure the above-mentioned requirements, an apparatus has been created. A removable mesh trap is installed at the bottom flush outlet of the mini-hydro power plant forebay tank and the debris which are discharged through the flush outlet is collected. It is noteworthy to mention that most of the collected floating debris are tree leaves and small sticks. The collected debris is weighed on an hourly basis and 10 such samples were collected. The noted wet weights of the hourly debris accumulation are then compared with the previous 6 hour and previous 12-hour catchment rainfall. The rain gauge located at “Kabaragala” which is within the catchment of “Moragaha Oya” is used to collect the relevant rainfall data. Figure 23 shows the installed debris collection apparatus and weighing of the collected debris.

Figure 23 : floating debris collection apparatus

3.4.2 Results

As stated in the methodology, the hourly weights of the floating debris are compared with the previous 6 hour and previous 12-hour catchment rainfall separately.

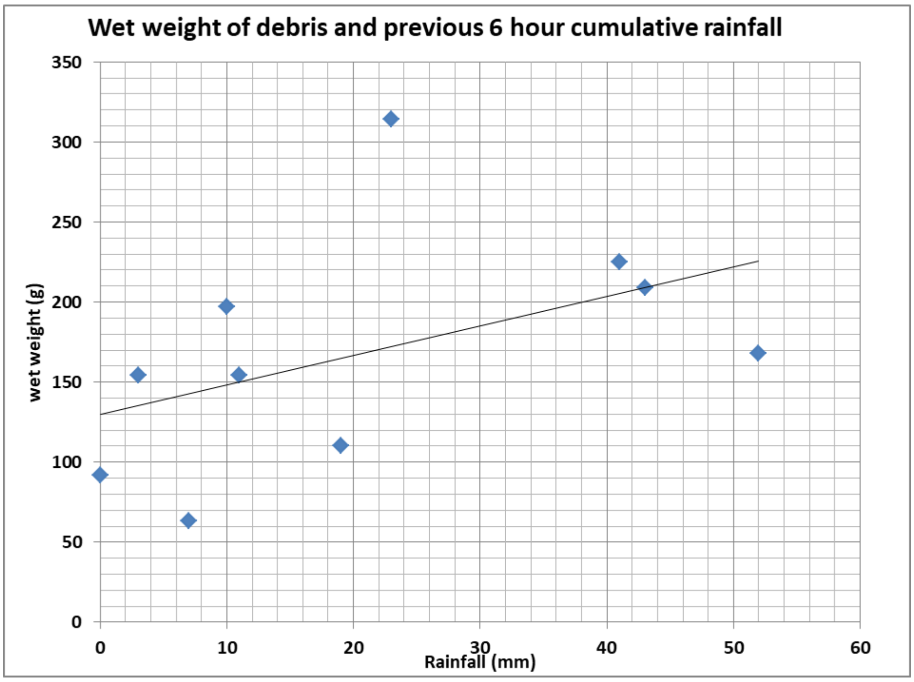

Figure 24 : hourly wet weight of the floating debriefs and previous 6 hour rainfall.

The result of the hourly floating debris weight and the previous 6-hour rainfall does not show a significant relationship (refer to figure 24). The linear trend line drawn according to the data points is lying almost in parallel to the x-axis.

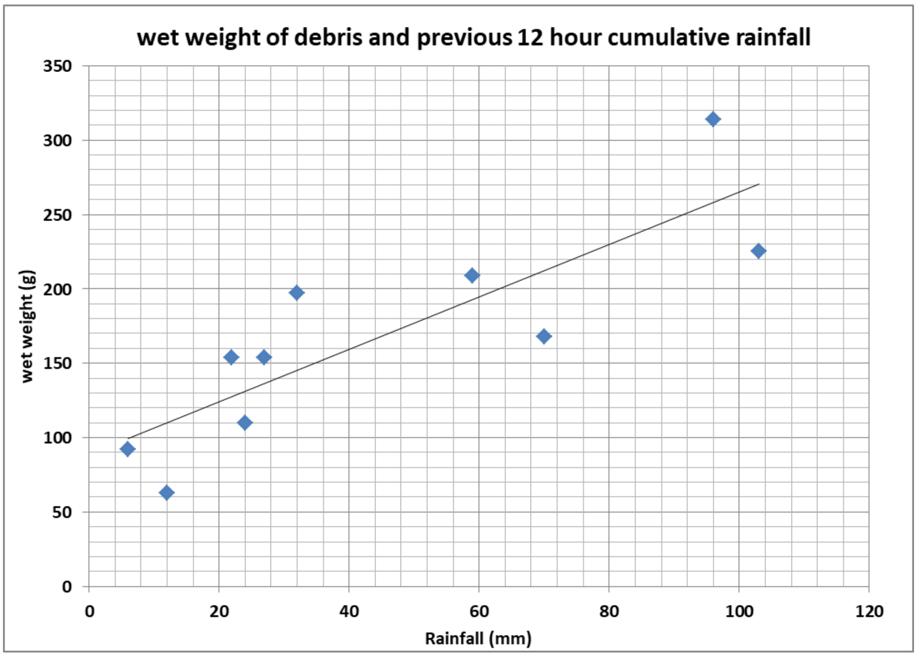

Figure 25 : hourly wet weight of the floating debriefs and previous 6 hour rainfall.

However, when referring to figure 25, the hourly wet weight of the floating debris and previous 12-hour rainfall show a significant relationship. The trend line lies through the data points in an equally distributed manner.

3.5 Finalized stream parameter relationships

In order to predict power plant output at various flow combinations with the stream parameter inputs, the availability of relationship with the selected inputs and powerplant output variation is to be confirmed. In order to achieve that Results of the previously discussed experiments were critically analyzed. The relationships listed in table 7 are selected to use in intelligent controller development.

Table 7 : Stream measurements which selected to use as inputs in intelligent controller

Measurement supposed to use as inputs to the intelligent controller	**Strem parameter which link with the measurement**
Turbidity	Quantity of micro particles - TDS
Turbidity	Quantity of micro particles - TSS
12-hour catchment rainfall	Quantity of floating debris

3.6 Overview of proposed intelligent controller software

In line with the objective of this study, inputs were selected based on experiment results in the previous section. An ANN is selected as the core component of the proposed intelligent controller because with the availability of a large number of known input and output data, a supervised training process can be employed. The supervised training of ANN is proven to be highly successful in output prediction [9]. On the other hand, the selected input data category has been used previously to address different problem statements in the same industry using the same ANN techniques [8],[9]. The basic design is to replace the existing fix lookup table (flow distribution table) of the power plant control system with a dynamic table that is updated by the intelligent controller. the rest of the control functions including maximization selection of the given flow range. Figure 26 shows the basic structure of the proposed flow distribution control system including the intelligent controller.

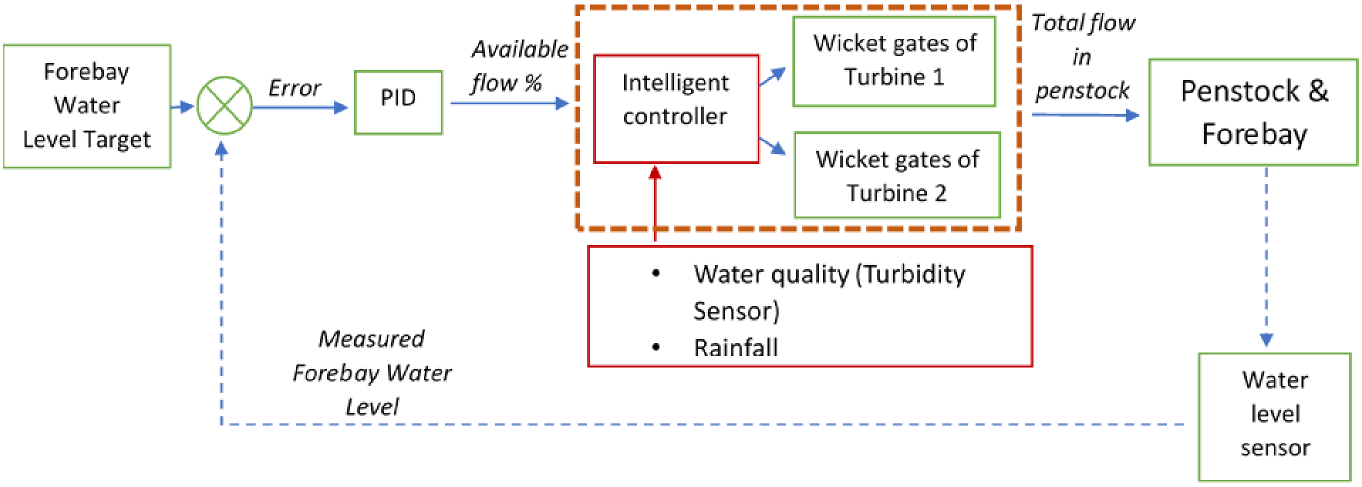

Figure 26 : Proposed flow distribution control system including intelligent controller.

3.7 Analyzation of data sample

According to the selected inputs and available outputs, there are 121 power output values (refer to table 2 and table 3) that have to be predicted by the intelligent controller for each set of inputs. Because there are 121 different flow combinations available at the existing flow distribution table. For an ANN-based system, it is nearly impossible to predict such a large number of data points. Also, designing the controller specifically for the “Moragaha Oya” mini hydropower plant control system will be a limitation to developing this controller as a general solution for any mini hydropower plant.

In order to reduce the output data set size and bring it to a more generalized form, a linear regression method is employed [11]. Linear regression is a basic and commonly used type of predictive analysis.

The overall idea of regression is to examine two things including whether a set of predictor variables do a good job in predicting a dependent variable and which variables, in particular, are significant predictors of the outcome variable, and in what way do they indicated by the magnitude and sign of the beta estimates impact the outcome variable.

These regression estimates are used to explain the relationship between one dependent variable and one or more independent variables. The simplest form of the regression equation with one dependent and one independent variable is defined by the formula y = c + b*x, where y = estimated dependent variable score, c = constant, b = regression coefficient, and x = score on the independent variable. In this case, 121 data points can be considered as values of the dependent variable of a 3-dimensional surface equation and the flow of each turbine can be considered as two independent variables. The total power output "y" at a given combination can be expressed as follows where x1 is the input flow of turbine 1 and x2 is the input flow of turbine 2, βkj are the coefficients supposed to be obtained from the linear regression model.

$$\mathrm{y} = \sum_{k=1}^{n} \sum_{j=1}^{n} \beta_{jk} x_1^{k-1} x_2^{j-1}$$

When the degree of the surface is limited down to 2, there will be a surface equation of 9 coefficients as below.

$$y = \beta_{11} + \beta_{21}x_1 + \beta_{12}x_2 + \beta_{22}x_1x_2 + \beta_{13}x_2^2 + \beta_{31}x_1^2 + \beta_{23}x_1x_2^2 + \beta_{32}x_2x_1^2 + \beta_{11}x_1^2x_2^2$$

The "fit" [11] function in the "Matlab" linear regression toolbox will be utilized to obtain above mentioned 9 coefficients at each data set and that 9 coefficients sets can be used as training data to the ANN of the intelligent controller. this way, the predictions of the ANN became a more accurate and also less computational burden to the central processing unit (CPU) of the power plant control computer. Figure 27 shows a such predicted surface and its coefficients of a set of data.

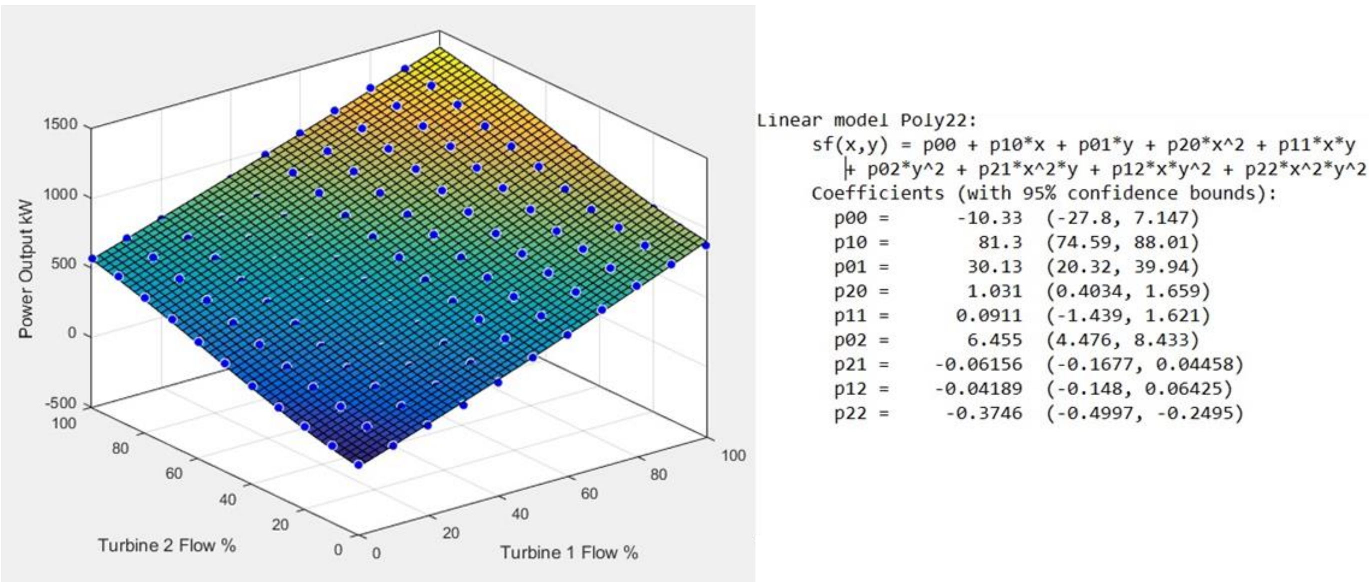

Figure 27 : Surface coefficients obtained from liner regression model.

3.8 Design process of ANN structure

To accept 2 variables as inputs and provide nine variables as outputs, it is obvious the ANN shall have two input variables and nine output variables. But the internal structure shall be designed in a way such that the ANN is capable of predicting desired outputs accurately [6]. There are two main internal structure variables namely the number of neurons in a hidden layer and the number of hidden layers. Selection of said parameters shall be done according to one of the flowing methods [7]

- Use of trial-and-error method
- Use of empirical rules
- Use an algorithm that dynamically adjusts the network configuration

The first two methods were adapted during the design process. The following empirical rules have been followed for the finalization of the number of hidden layers.

- Number of hidden layers shall be between the input and output layer size
- Number of hidden layers shall be set to something near (inputs +outputs) * 2/3
- Number of hidden layers shall never larger than twice the size of the input layer

Accordingly, 3 simulations were carried out using 100 sets of data, and in each simulation number of hidden layer neurons ware set at 1, 3, and 4 respectively. The training performance ware evaluated using the "Matlab" ANN tool and the RMS error [6] is recorded at each simulation. Figure 28 shows the simulation results.

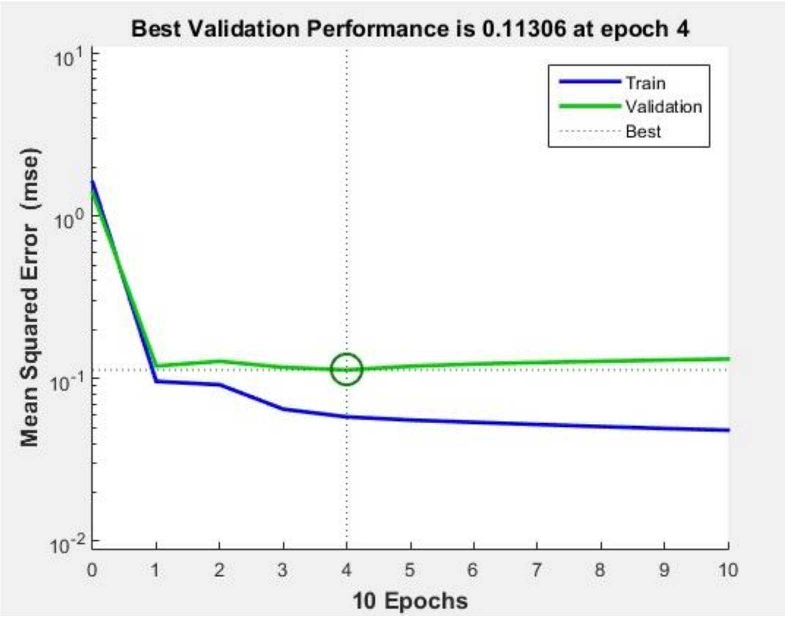

ANN with 1 hidden layer

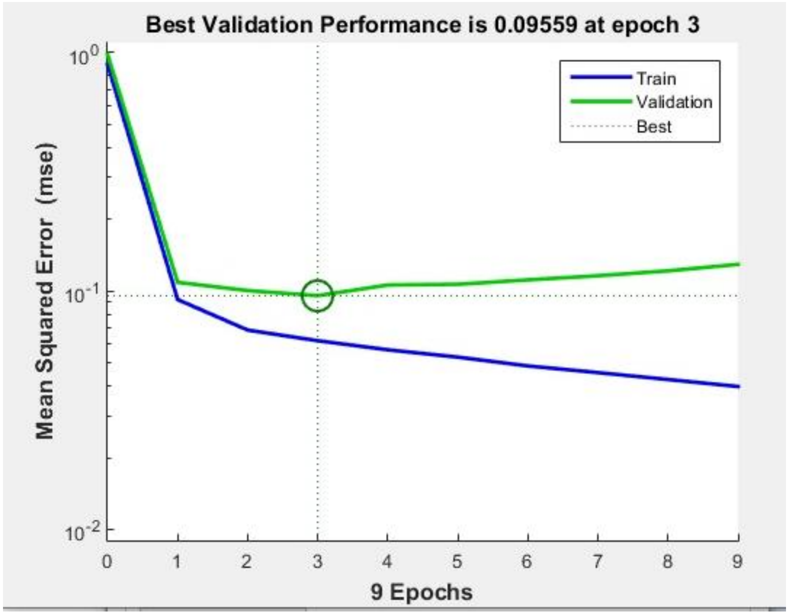

ANN with 3 hidden layers

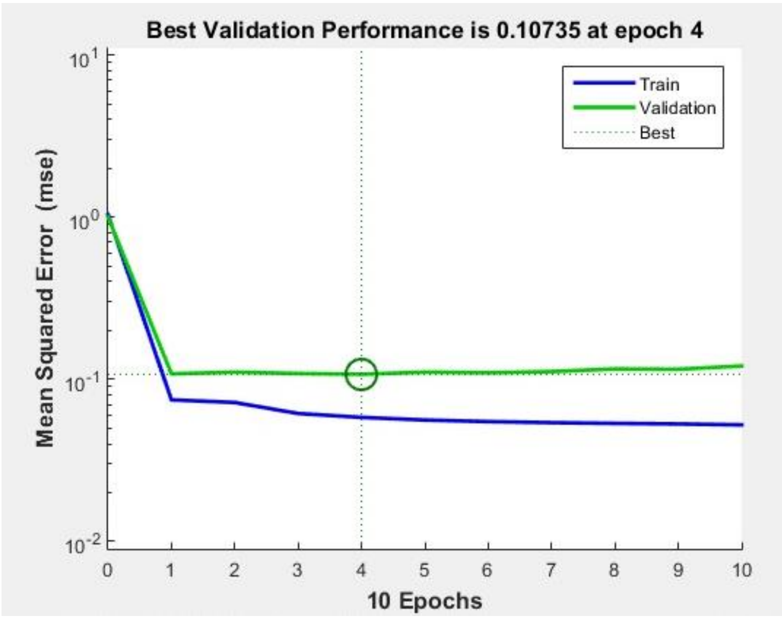

ANN with 4 hidden layers

Figure 28: ANN training simulation for different hidden layers.

According to the simulation results, ANN with 3 hidden layers has been shown the least value for RMS error. Hence that structure is selected to use in the proposed intelligent controller. the finalized code will execute in the following order starting from the reduction of input data using linear regression and followed through the ANN creation, training, and validation (refer to figure 29). once the ANN is trained and finalized, the trained network can be directly imported to the intelligent controller for continuous use.

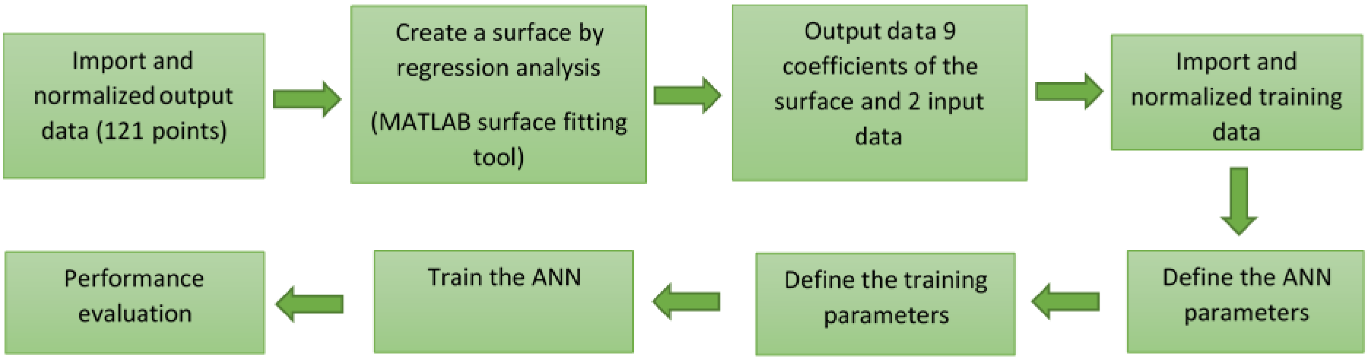

Figure 29 : Steps of ANN implementation.

3.9 Software development of intelligent controller.

As explained in the previous chapter the finalized and trained ANN will be used in continuous operation as the core of the intelligent controller. During the continuous operation, the ANN will receive input data from the operator and the sensor. Thereafter the ANN will provide the 9 coefficients of the flow distribution table predicted according to the flow condition. The 121 output data points will be created using the surface equation and the same will be updated in the lookup table of the flow distribution control loop. The operation procedure of the proposed intelligent controller is shown in figure 30. The intelligent controller software is developed in "Matlab" and some of the existing functions of the power plant control software are linked to this intelligent controller software.

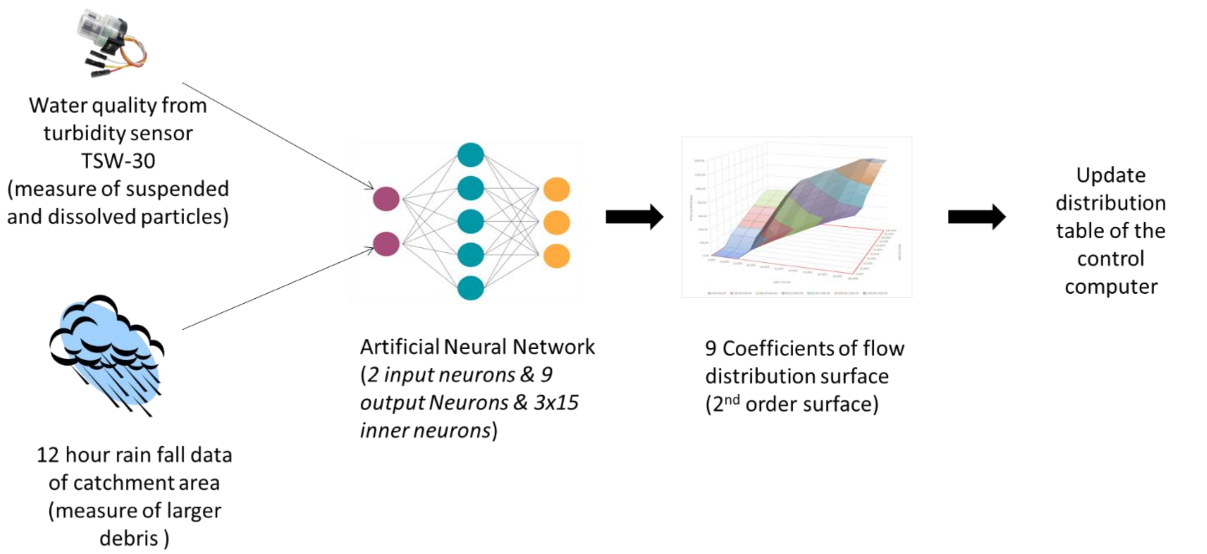

Figure 30: Operations procedure of the intelligent controller.

3.9.1 Training data collection interface

A vital function of the intelligent controller software is to collect as much as possible data which will be used to train the ANN. In this case, data need to be collected during various flow conditions. Said data includes turbidity sensor reading, previous 12-hour rainfall, and power output of the mini hydropower plant at all possible flow combinations. To collect power output data, the power plant has to operate throughout the all-possible flow combinations. if A power plant operator is employed to collect all power output data, there might be faulty data due to human errors. To mitigate these errors, a simple user interface is developed for the power plant operator to execute the training data collection function. In this interface, the operator has to manually enter the rainfall data. thereafter with a press of a button turbidity sensor reading and the power plant output data will be recorded as training data. The existing “Seek” function of the power plant control system is used to collect the output data at all flow combinations. Figure 31 shows the developed training data collection interface that appears on the power plant control computer. The power plant operators were instructed to collect data twice a day using this interface.

Figure 31 : Training data collection interface.

3.9.2 Continues operation interface (to update flow distribution control table)

The main function of the intelligent controller is to update the flow distribution table based on inputs during continuous operation. Another interface developed is attached to intelligent controller software which facilitates the operator to update the flow distribution table. Operators have to manually update the previous 12-hour rainfall data and the turbidity sensor reading is linked to this interface as real-time input. Apart from that, this interface also views the ANN-generated flow distribution surface equation and the surface shape. The 121 power output data points will be generated using this surface and the same will be updated on the existing flow distribution control loop. Figure 32 shows the developed interface to update the flow distribution table.

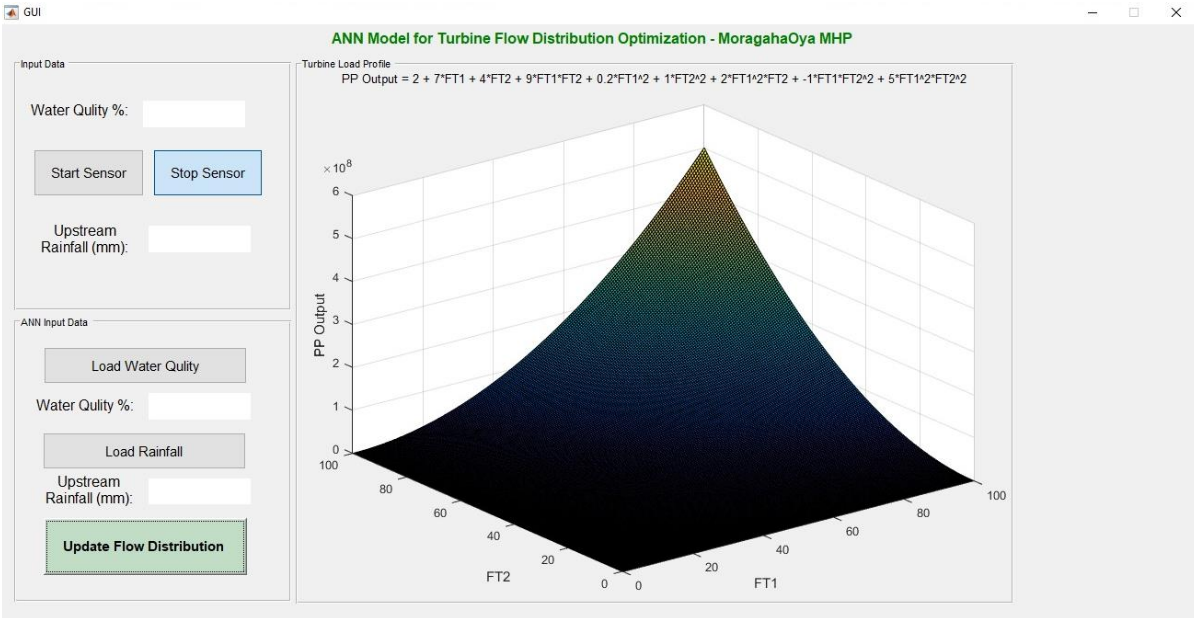

Figure 32 : Continues operation interface.

4. DESIGN AND INSTALLATION OF ADDITIONAL HARDWARE IN THE MINI HYDRO POWER PLANT

As mentioned in chapter 2.3, Moragaha Oya mini hydropower plant has been selected as the study site for this research. The power plant control system is implemented on a "Pro-face 4300" embedded computer with a "Windows" operating system. The physical inputs and outputs are routed through the "Beckhoff" input and output PLC interface which is connected to the embedded computer via the "TwinCAT" communication protocol. Due to this arrangement, turbidity sensor readings can be fed into the intelligent controller installed in the embedded computer using the same channel. In addition to that, the flow intake of each turbine is and the total output power of the power plant also possible to link to the intelligent controller within the software level.

The turbidity sensor has been installed in the forebay which is 1.4km away from the powerhouse. Therefore, the signal needs to travel all the way down to the powerhouse. In order to achieve that, the hardware arrangement shown in figure 33 is designed and installed in the forebay areas and the powerhouse. The two areas are already connected with a multi-core shielded control cable for the water level data acquisition. A remaining core of said control cable has been utilized to transfer turbidity sensor signals. Adequate signal conditioning, surge protection, and electrical isolation are also provided since the control cable has been drawn along with the penstock pipe in an open area with a high keraunic level.

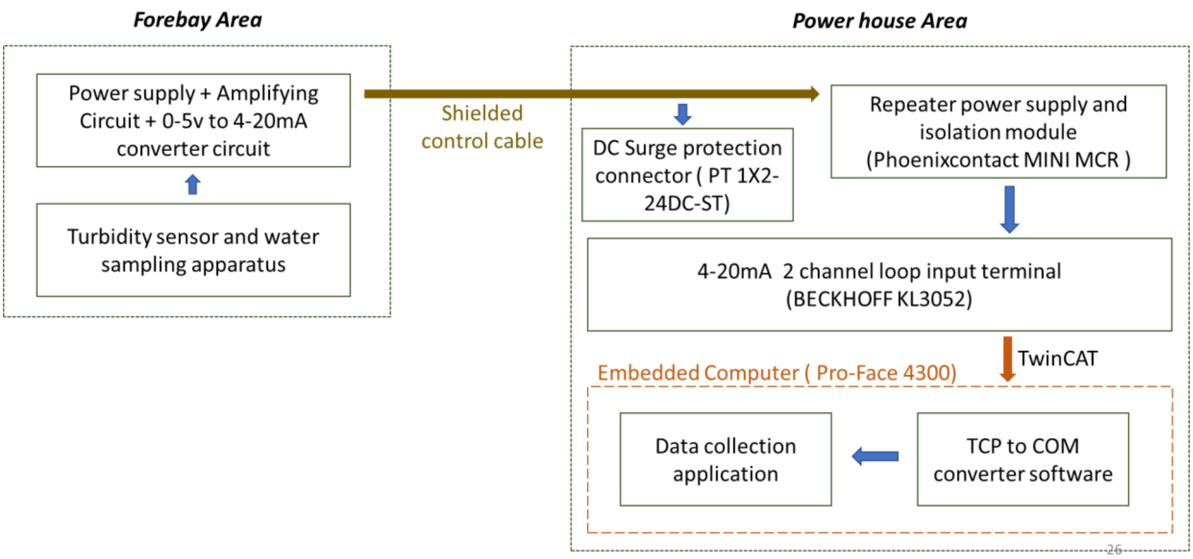

Figure 33 : Hardware arrangement.

4.1 Additional hardware in forebay area

The hardware items which are described in this chapter have been installed in the forebay area in order to read the turbidity level of the intake water, signal conditioning, and amplification. A separate pipeline has been erected to sample water from the forebay tank and run through the turbidity sensor. Figure 34 shows the installed hardware components at the forebay with sensor mounting apparatus which allows sampling water flows through the turbidity sensor.

Figure 34 : installed hardware at the forebay.

4.1.1 Turbidity sensor

There are several accepted measurements methods are available for the turbidity of the water. Among them, the propensity of particles to scatter a light beam focused on them is now considered a more meaningful measure of turbidity in water [12]. Turbidity measured this way uses an instrument called a nephelometer sensor with the detector set up to the side of the light beam. More light reaches the detector if there are many small particles scattering the source beam than if there are few. The units of turbidity from a calibrated nephelometer are called Nephelometric Turbidity Units (NTU). To some extent, how much light reflects for a given number of particulates is dependent upon the properties of the particles like their shape, color, and reflectivity.

“TSW-30” is a sensor that operates according to the above principle. Additionally, this sensor provides both analog and digital outputs depending upon the requirement. This sensor is designed to operate in a wide NTU range and very low response time. Due to its robust characteristics, TSW-30 is utilized in this project. Table 8 provides the Basic Characteristics of the TSW-30 turbidity sensor.

Table 8 : Basic Characteristics of TSW-30.

Parameter	**Range**
Operating Voltage	5.00V DC
Nominal Current	40mA
Response time	<500ms
Insulation resistance	100MΩ
Operating temperature	20°C-90°C
NTU Range	0-1000 ±30
Photo Emitter wavelength	940nm
Analog output	0-5 V
Digital output	0/5 V low/high

Figure 35 shows the output characteristics of the turbidity sensor TSW-30 at 25 °C temperature.

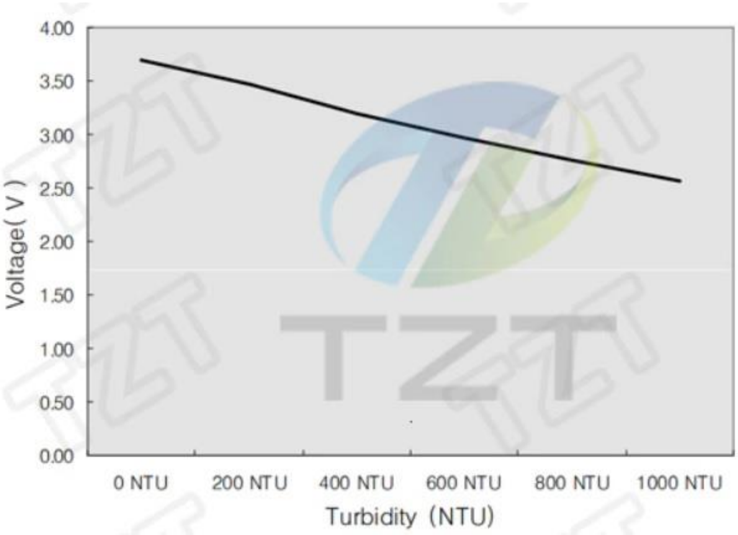

Figure 35 : installed hardware at the forebay

4.1.2 Signal convertor

The turbidity sensor output signal shall be transmitted to the powerhouse which is located 1.4km downstream of the forebay. Therefore, the analog voltage output signal has been converted to 4-20mA standard current signal which can be transmitted to long distance via shielded copper cable without signal distortion. In order to chive that a signal conversion and amplification module is used with the turbidity sensor.

The module consists of LM 324 and LM317 integrated circuits which provide the amplification and voltage signal to current signal conversion. In addition to this module, a 230V/5V switch mode power supply, and circuits breaker for overcurrent protection.

4.2 Additional hardware in power house area

The converted signal is transmitted through the control cable and shall be connected to the existing PLC input interface of the embedded computer. In order to achieve that takes, a set of additional hardware has been installed in the powerhouse as described below sections.

4.2.1 DC surge arrestors

Due to the long distance between the forebay and the powerhouse, the control cable may be subjected to surge induces due to nearby lightning strikes. If such a surge enters the input interface, the whole control system is at risk of damage due to surge voltages. In order to prevent that DC surge arrestors have been installed at the termination end of the control cable.

“BXT ML2 BE S 24” DC low voltage surge protector is a known device specially used in long-distance copper telecommunication cables. The same device is utilized in this project. Figure 36 shows the installed DC surge arrestors in the power plant control cabinet. Basic characteristics of the surge arrestors are also mentioned in table 9.

Table 9 : Basic Characteristics of BXT ML2 BE S 24.

Parameter	**Range**
Nominal voltage	24 V
Nominal current	0.75 A
Total lightning impulse current (10/350 μs)	9 kA
Total nominal discharge current (8/20 μs)	20 kA
Series resistance per line	1.8Ω

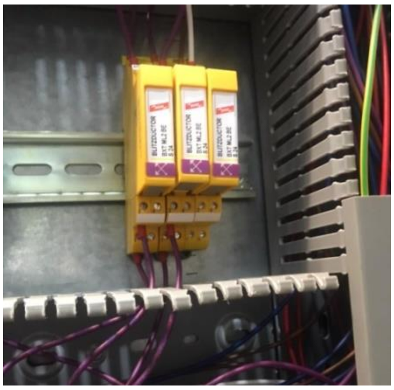

Figure 36 : DC Surge arrestors.

4.2.2 Repeater power supply

The 4-20mA signal loop needs to be powered and electrically isolated from the PLC interface to ensure safety from surges. A “PHONIX CONTACT-MINI MCR” repeater power y and isolation module is used to achieve said purpose. this repeater power supply supplies transmitters in the field and electrically isolates the input signal from the output signal. The module can be used in both isolator and repeater power supply operations. Electrically isolated 0-20 mA or 4-20 mA analog standard signals are available on the input and output sides. The power supply (19.2 V DC to 30 V DC) can be supplied via connection terminal blocks on the modules or in conjunction with the DIN rail connector.

Table 10 provides the basic characteristics of the repeater power supply and figure 37 shows the installation of the repeater power supply in the power plant control cabinet and the connection diagrams.

Table 10 : Basic Characteristics of PHONIX CONTACT-MINI MCR.

Parameter	**Range**
Current input signal	4-20mA
Input resistance current input	50 Ω
Transmitter supply voltage range	14.7 V -25.5 V DC
Current output signal	4 mA ... 20 mA
Transmission Behavior	1:1 to input signal

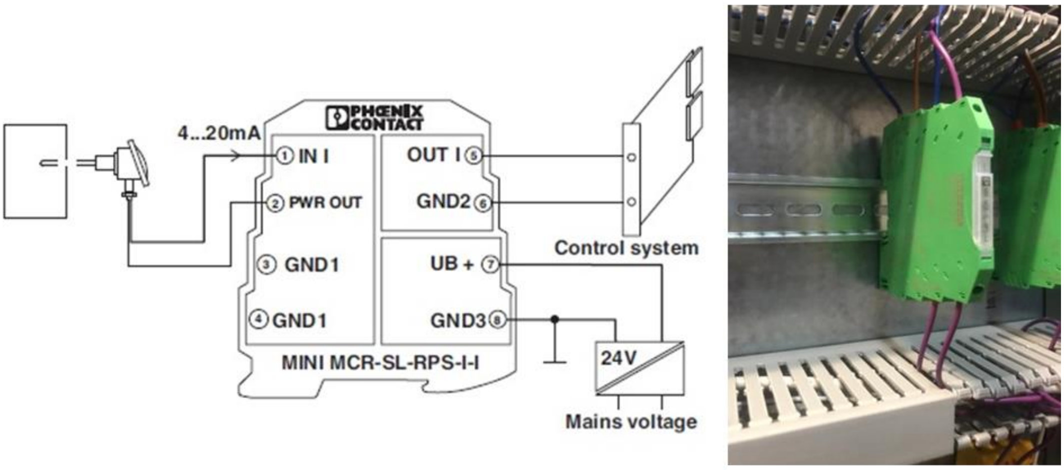

Figure 37 : Repeater power supply.

4.2.3 Wicket gate position sensor

he input flow to each turbine is needed as a feedback signal to the flow distribution control system as well as to the training data collection tool. This measurement is taken as the wicket gate opening of each turbine and then converted to the intake flow since the water head is constant at the forebay. The full moving stroke of the linear servo motor which drives the wicket gates is about 100mm. hence to achieve the required level of readings, the sensor shall be cable of reading a 1mm movement of the linear servo motor. High repeatability of the readings is also a must requirement to collect a large number of training data. Therefore to improve the resolution and the repeatability of the measurement, the existing linear potentiometer sensor is changed to a more accurate sensor.

“Temposonics-EL” high precision Magnetostrictive linear position sensor is used as the new wicket gate position sensor. The sensor can be directly replaced without any signal modifications since this sensor comes with on board 4-20mA converter module. The absolute, linear position sensors rely on magnetostrictive technology, which can determine position with a high level of precision and robustness. This sensor consists of a ferromagnetic waveguide, a position magnet, a strain pulse converter, and supporting electronics. The magnet, connected to the object in motion in the application, generates a magnetic field at its location on the waveguide. A short current pulse is applied to the waveguide. This creates a momentary radial magnetic field and torsional strain on the waveguide. The momentary interaction of the magnetic fields releases a torsional strain pulse that propagates the length of the waveguide. When the ultrasonic wave reaches the end of the waveguide it is converted into an electrical signal. Since the speed of the ultrasonic wave in the waveguide is precisely known, the time required to receive the return signal can be converted into a linear position measurement with both high accuracy and repeatability.

Figure 38 shows the newly installed wicket gate position sensor and table 11 give the basic characteristics of the Temposonics-EL linear position sensor.

Table 11 : Basic Characteristics of Temposonics-EL linear position sensor.

Parameter	**Range**
Resolution	Infinite
Repeatability	≤ ±0.005 %
Operating voltage	24 V DC
Stroke length	254 mm
Output	4-20mA

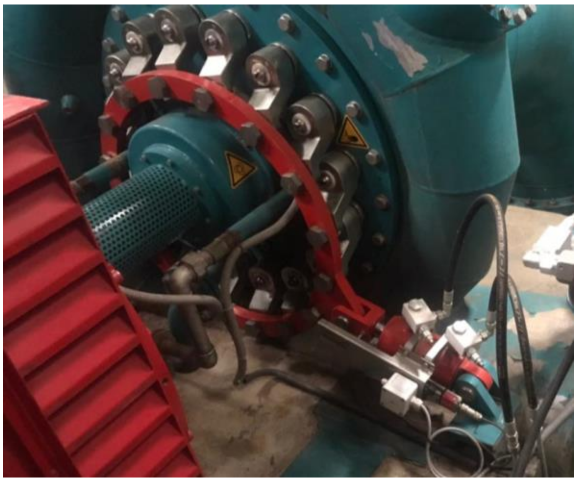

Figure 38 : Wicket gate position sensor

4.2.4 Analog input module

The input signals from the turbidity sensor and the wicket gate position sensor shall be fed into the embedded computer via its PLC interface. A multi-channel analog input card is installed to the existing input, output array.

As this control system utilized the “Beckhoff” PLC interface and EtherCAT data communication bus, the KL3052 2-channel loop-powered analog input terminal is used to feed the said input data. The job of the KL3052 analog input terminal is to supply power to repeater power supplies located in the control cabinet and to transmit analog measurement signals with electrical isolation to the automation device. The voltage for the sensors is supplied to the terminal via the power contacts. The power contacts can optionally be supplied with operating voltage in the standard way with electrical isolation. The input electronics are independent of the supply voltage of the power contacts. The 0 V rail is the reference potential for the inputs. The run LEDs give an indication of the data exchange with the Bus Coupler. The error LEDs indicate an overload condition and a broken wire.

Figure 39 shows the KL 3052 installed in the existing PLC array and Table 12 provides the basic characteristics of the KL3052

Table 12 : Basic Characteristics of KL3052 analog input module.

Parameter	Range
Resolution	12 bit
Input	4-20mA
Operating voltage	12 V DC
Communication	K bus
Internal resistance	80Ω

Figure 39 : analog input module

4.3 Embedded Computer

The existing "Pro-Face 4700" embedded computer is utilized to run the intelligent controller software. TCP to COM converter software is also installed in this computer for feeding the data to the intelligent controller software. The "Wassi Systems" power plant control software, "Twin-Cat" PLC interface software, and "Marelli MEC -100" voltage and power factor control software are also installed on this computer. Table 13 shows the basic characteristics of the embedded computer.

Table 13 : Basic Characteristics of "Pro-Face 4700" embedded computer.

Parameter	**Range**
CPU	AtomZ510 1.1 GHz 512 KB L2 cache
RAM	2GB DDR2 400 MHz
Ethernet Interface	RJ-45 Modular jack
Rated Voltage	24V
Operating System	Windows® Embedded Standard 2009

5. RESULT AND DISCUSSION

Once all hardware and software setup is completed, training data collection is started. There was a large number of data points have been collected throughout the northeastern monsoon period and the inter monsoon period. Thereafter the ANN was trained and the intelligent controller was engaged for actual operations. Depending on the results, further modifications to the ANN have been conducted and the ANN training is also conducted. This chapter explains the process of ANN training and the performances validation of the proposed intelligent controller.

5.1 Training of the intelligent controller

When it comes to the training preperformance of the intelligent controller, A thorough analysis has been conducted to select the training data set which provides the lowest validation RMS error which is used as the deciding factor of the best data set. Because the main goal of training a neural network is to perform well on unseen examples, not on raining examples. If the learning rate is small enough, then training a neural network with too many epochs will result in loss converging to one of its local minima since at every epoch the coefficients are moving towards minimum. Once a minimum is reached, then further training will not change the loss since the parameters are updated at a minimum. In other words, the parameters which are close to zero do not change.

However, in most cases, the loss function is not required to reach its minimum value since that would result in a neural network that is more prone to overfitting. The loss function is a measure of how well the neural network does on the training set [13]. If the loss is minimized beyond a certain point, then the neural network is likely to do worse on the unseen examples and the neural network will have poor generalization performances. As the number of epochs increases, at first, both the training error and the test error starts decreasing, but after a certain point, the test error starts to increase (the training error continues to decrease since the training method is set to minimize the training error) As shown in figure 40.

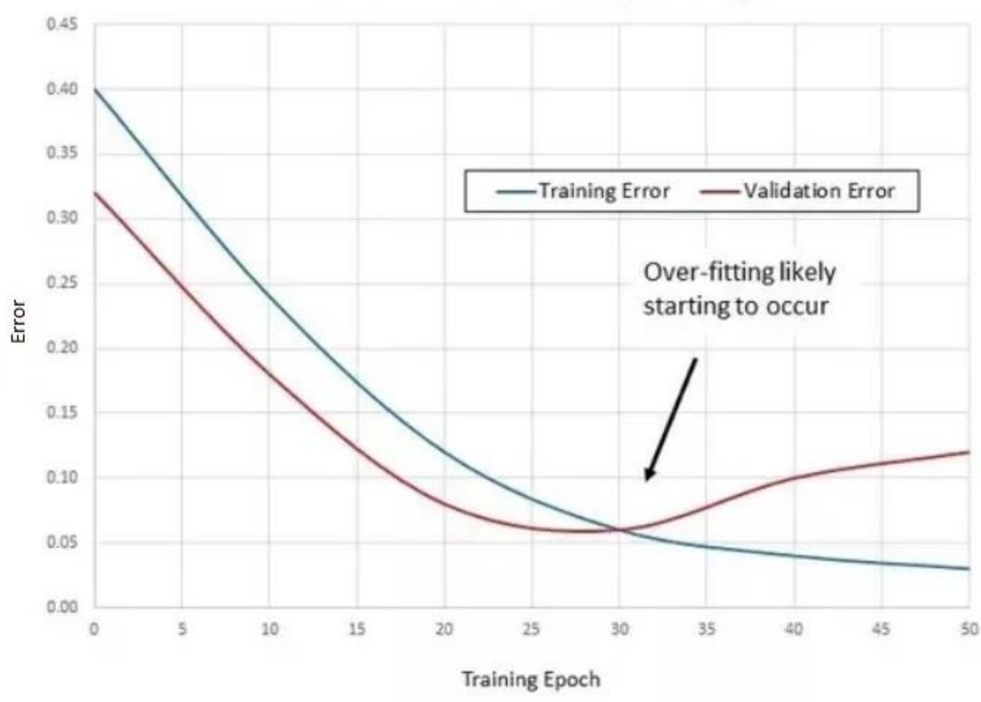

Figure 40 : Variation of Training Error and Validation Error

Compression of the ANN output and the desired validation data point of each flow distribution surface coefficient is conducted along with the validation RMS error. The first training is done for 118 data points. During the evaluation of the results, validation has been conducted to separate 100 data points. thus, the ANN output does not show a proper correlation with its validation data for the first coefficient of the flow distribution surface as shown in figure 41. The validation RMS error is also high and the results of the validation are mentioned in table 14. Because of the poor performances, It is decided to increase the training data and perform another validation.

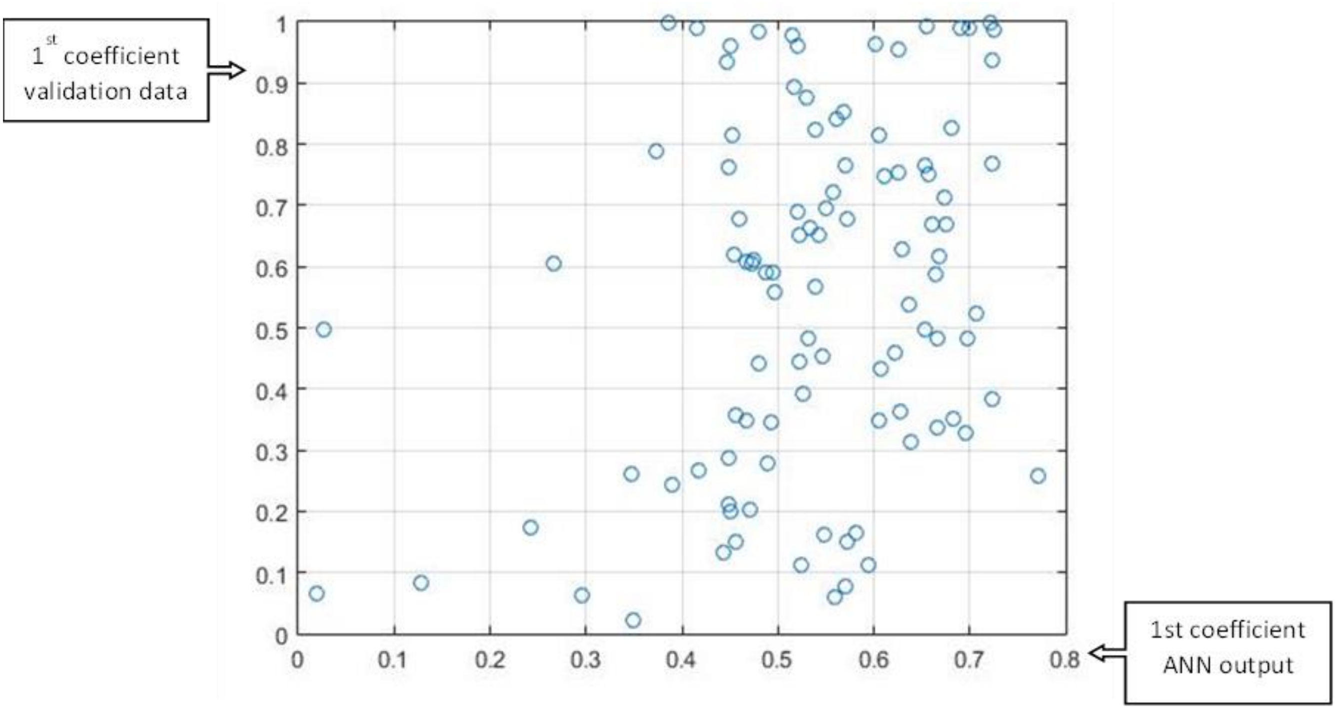

Figure 41 : RMS Error Training and Validation for 118 data points

Table 14 : ANN training performances with 118 data points

Training Parameter	**Value**
No of Training data points	118
No of Validation data points	100
No of Epoch	1000
RMS Training Error	0.1583
RMS Validation Error	0.2758

During the next ANN training event, the training data has been increased to 531 data points. In this training event, the ANN output shows a proper correlation with its validation data for the first coefficient of the flow distribution surface as shown in figure 42. The validation RMS error was also reduced and the results of the validation are mentioned in table 15. As this training session shows more improved results, the intelligent controller has been deployed for the continues operation and the power plant performances are not improved (will be explained in chapter 7.2) therefore it is decided to conduct another training event with the changes to the ANN structure and addition of more data points from the mid-power operation region if the power plant.

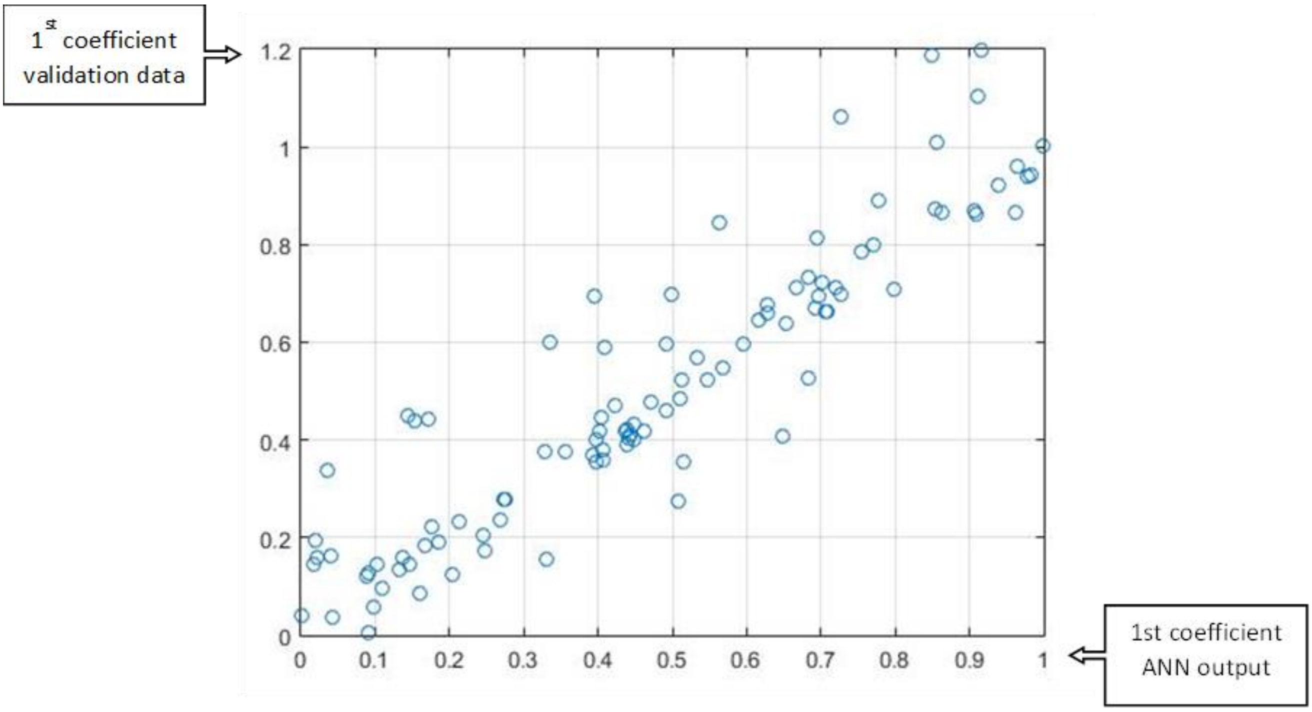

Figure 42 : RMS Error Training and Validation for 531 data points

Table 15 : ANN training performances with 531 data points.

Training Parameter	**Value**
No of Training data points	531
No of Validation data points	100
No of Epoch	1000
RMS Training Error	0.0861
RMS Validation Error	0.1197

During the 3rd ANN training event, the training data has been increased to 723 data points and the structure of the hidden layer neurons of the ANN is also improved. In this training event, the ANN output shows a much more improved correlation with its validation data for the first coefficient of the flow distribution surface than the previous cases as shown in figure 43. The validation RMS error was also reduced further and the results of the validation are mentioned in table 16. Also, the intelligent controller with this ANN shows the improved power output of the mini hydropower plant.

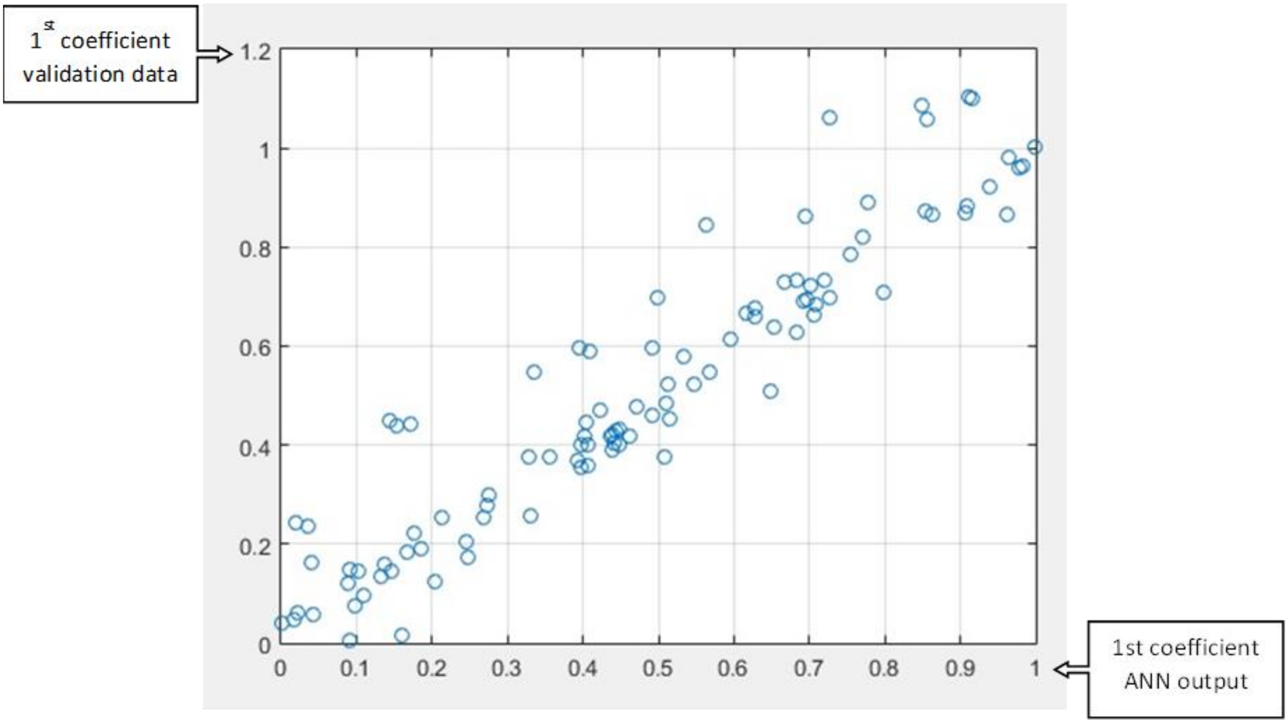

Figure 43 : RMS Error Training and Validation for 723 data points

Table 16: ANN training performances with 723 data points.

Training Parameter	Value
No of Training data points	723
No of Validation data points	100
No of Epoch	1000
RMS Training Error	0.0416
RMS Validation Error	0.1048

However, it is clear that the rate of reduction of RMS validation error is reducing at this point indicating that the ANN tends to get overfit. Therefore, it is decided to use above trained ANN for the intelligent controller performance validation.

5.2 Performance validation of the intelligent controller

5.2.1 Improvements in the output power

After proper ANN training, the intelligent controller is deployed to continues operation for 30 days in the power plant. The operators were instructed to perform the flow distribution control table update at every 6-hour interval. The controller performances were monitored at each output level for the clear water condition and the muddy water conditions separately. The results have been compared with the outputs of the existing fix lookup table and the expected theoretically calculated outputs. The turbines were ramped up with available river flow using both an intelligent controller and the fix lockup table during this exercise.

The first set of performance validation data is taken for the 531 data point trained ANN. The results are shown in figure 44 and figure 45 for the clear water and the muddy water respectively.

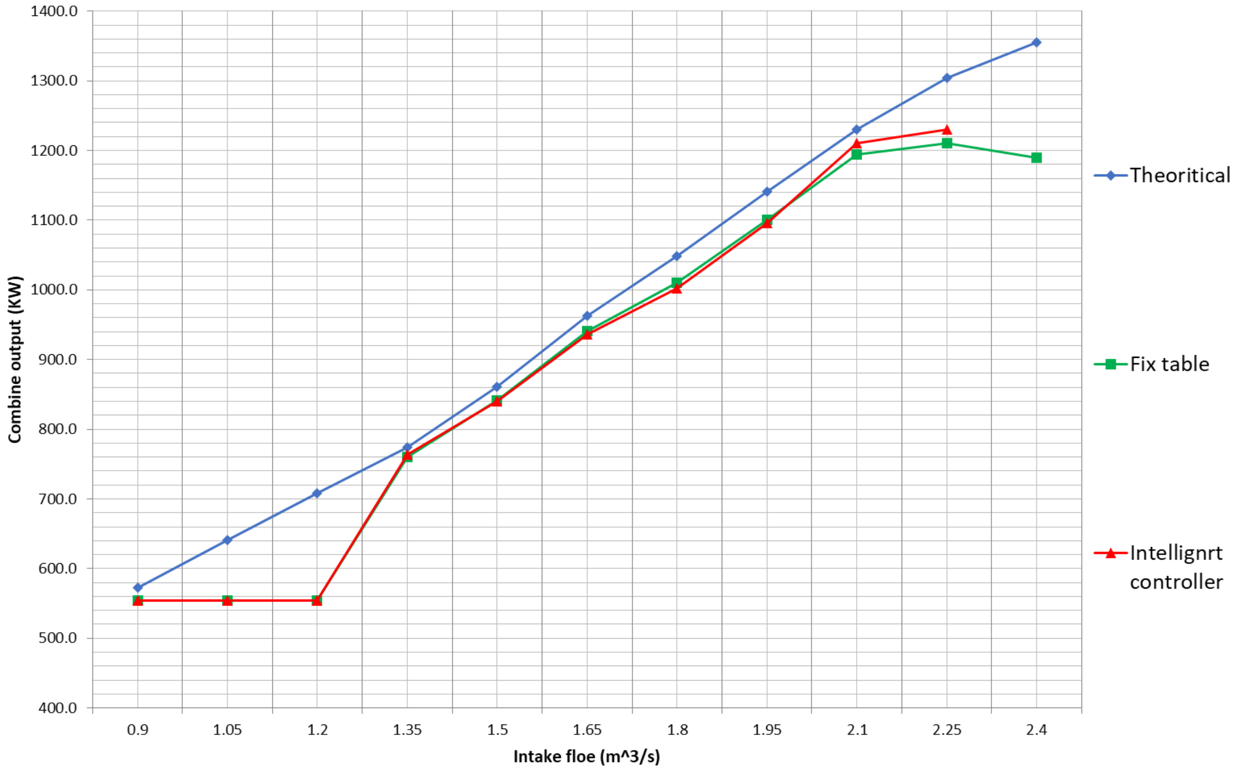

Figure 44 : Performance validation – ANN trained with 531 data points, operating in clear water

As per figure 38, the intelligent controller shows improved performances at the full load of the power plant. It does not allow to drop the output beyond 1230 kW when reaches 100% flow while the output drops to 1210kW at 90% flow and further to 1190kW at 100% flow when the power plant operates with fix lockup table provided operating points. But there is no significant improvement in the 50%-80% flow region with the intelligent controller. in fact, there is a reduction of output 70%-80% flow region with the intelligent controller during clear water situation.

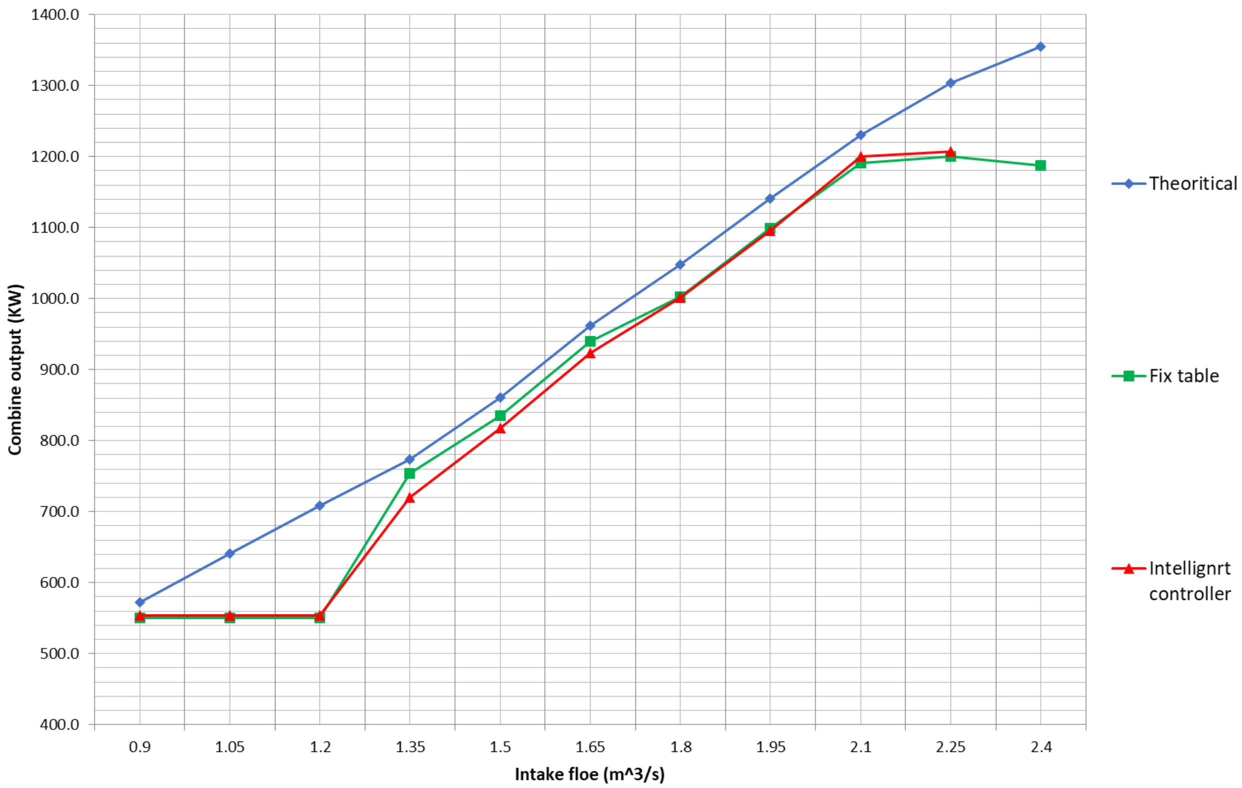

Figure 45 : Performance validation – ANN trained with 531 data points, operating in muddy water

As per figure 39, the intelligent controller performances get even poorer with muddy water conditions. The power plant reaches a maximum output of 1207kW at a 95% flow range which is only a 7kW increment from the respective fix table output. Also, during the 50%-75% flow range the intelligent controller output drop more than 30kW from its respective fix table output.

By looking at this performance, there were two possible conclusions that can be derived. The ANN is not trained sufficiently and the internal structure of the ANN is not specified properly. Therefore, more training data points were collected especially from the mid-flow region of muddy water operations where the total number of training data points is becoming 723. Also, the inner layers of the ANN are changed (explained in chapter 5.3). the retrained and re-structured ANN is programmed to the intelligent controller and again deployed for normal operation for 45 days. The results are shown in figure 46 and figure 47 for the clear water and the muddy water respectively.

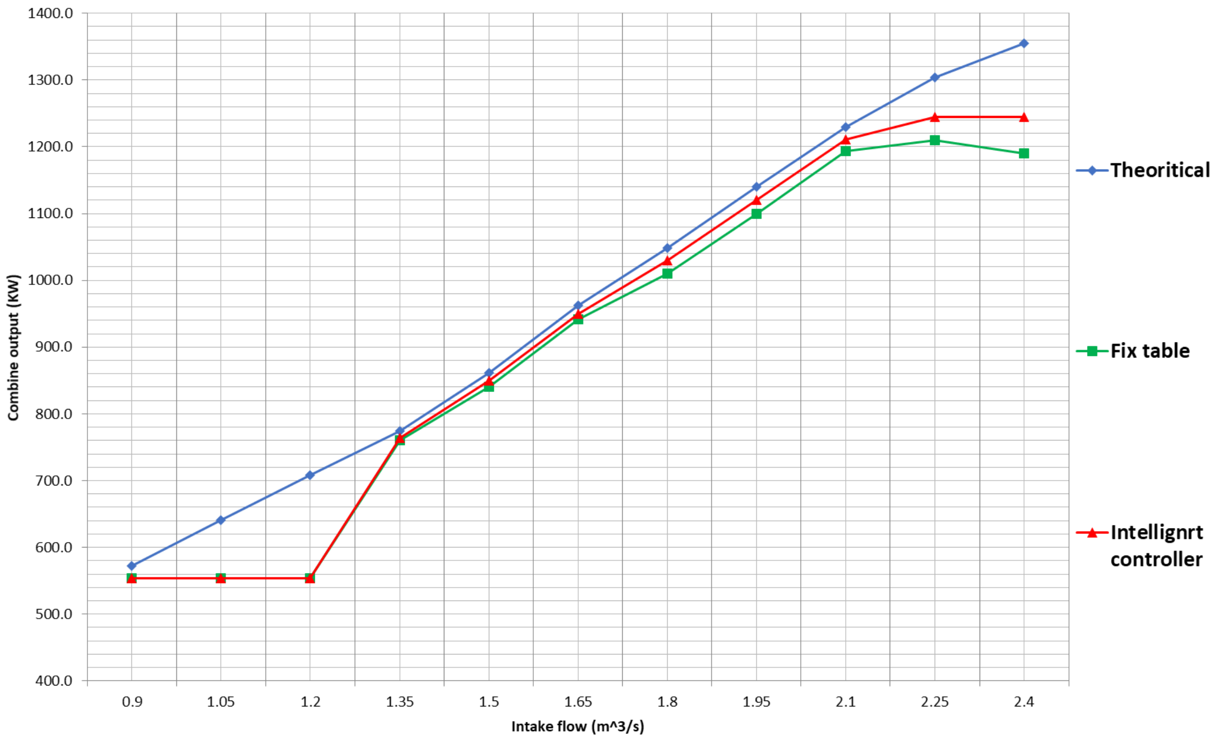

Figure 46 : Performance validation – ANN trained with 723 data points, operating in clear water

The improved controller now shows the expected results and the controller proposed operating points reach the maximum power plant output to 1245kW which is a 35kW improvement from the previous fix table capability. Apart from that, the overall performance improvement at 50%-100% flow region is notable.

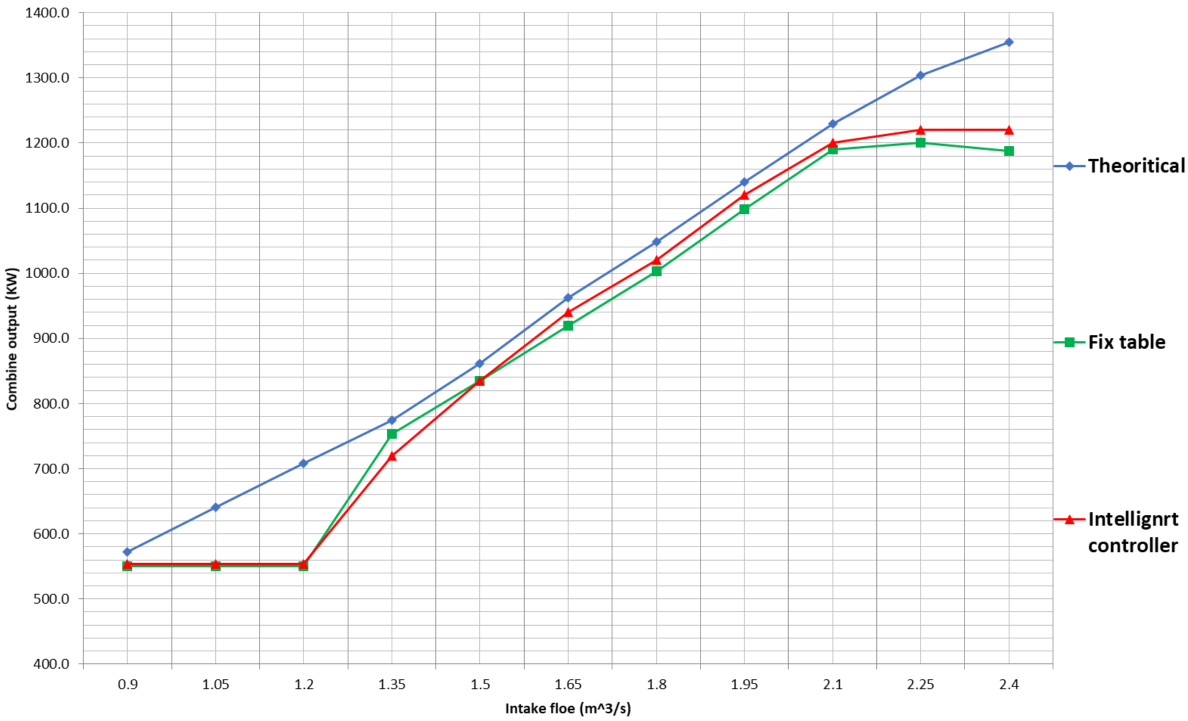

Figure 47 : Performance validation – ANN trained with 723 data points, operating in muddy water

Even though there is a slight output reduction at 50% flow region during muddy water operation, it is noteworthy that the overall performances of the intelligent controller are satisfactory for the muddy ware operation as well. The controller is able to reach 1220kW maximum output and maintain it from 90%-100% flow region which is a 20kW improvement from the maximum output of the fixed table during muddy water operation.

5.2.2 Improvements in the energy harvest

Even with the improved power output capabilities of the intelligent controller, there are some flow regions where the fixed table operates better than the intelligent controller. therefore, is it vital to analyze the changes in the overall daily energy harvest of the power plant. Thus, the daily average energy harvest of the power plant data for 47 days was also collected for the performance validation purpose. During this analysis, different daily rainfalls were considered to validate the performance of the intelligent controller in a more generalized manner. The results are shown in figure 48.

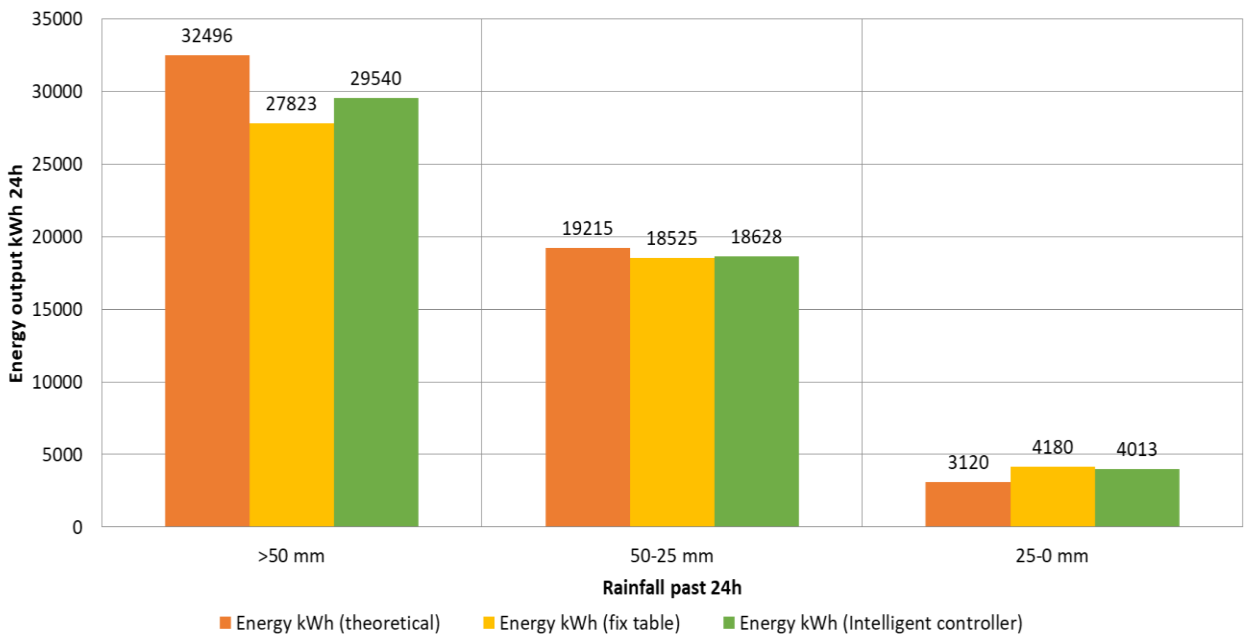

Figure 48 : Performance validation – Daily energy harvest for different daily rainfall levels.

As per the results, the best-improved energy harvest shows in the >50mm daily rainfall instances. The energy harvest of the 50mm-25mm instances also shows significant improvements. But during dry days (where the daily rainfall is 25mm-0mm) the energy harvest to not improve with the intelligent controller. this is mainly because of the limitation of the combined turbine operation due to lack of water. During this period the power plant is limited to single turbine operation most of the time. Also, the continued operation of the power plants is interrupted during these dry days due to a drop of water flow below 0.25m3/s (the small turbine can't operate blow 0.25m3/s flow due to mechanical limitations). But in general, there is a notable improvement of the daily energy harvest with the developed intelligent controller.

5.3 Prediction of expected Financial Gain

As explained in the previous chapter, there is a small loss in the generation when the intelligent controller is deployed on dry days. Therefore, a separate validation shall carry out to justify the said energy loss. Thus, a finance gain prediction for a one-year period has been conducted, and from the results, two possible operation possibilities are identified and described in this chapter.

Since there is a difference in energy harvest for each rainfall category, the occurrence of such a day in a given year is predicted. Since the power plant is commissioned in 2017, the Previous 4-year rainfall data of the catchment is only available. That data is used to calculate the average days of the occurrence of rainfall in each rainfall group. The calculation is presented in Table 17.

Table 17 : Prediction of rainfall occurrence in a year

	Occurrence of rainfall in past 4 years		
	0mm-25mm	**25mm-50mm**	**>50mm**
Days of occurrence in Last 4 years	951	221	289
% Of occurrence in last 4 years	65%	15%	20%
Average predicted occurrence of days /year	238	55	72

Using above data, a calculation has been done to find the financial gain (or loss) which can be expected by operating the power plant with intelligent controller throughout a year. The validation data from previous chapter is use to determine the energy gain (or loss) in each rainfall segment. The results of the calculation are mentioned in table 18.

Table 18 : Predicted financial gain for continues operation of intelligent controller for a year

Rainfall/day mm	**Additional generation /day kWh**	**Average occurrence days /year**	**CEB feed in tariff LKR/kWh**	**Estimate gain LKR/year**
0mm-25mm	-167	238	17.75	-705,491.50
25mm-50mm	103	55		100,553.75
>50mm	1717	72		2,194,326.00
Annual Predicted Gain LKR				**1,589,388.25**

There is another operation possibility that the power plant is operated with the intelligent controller for the days where the rainfall is higher than 25mm and use the fixed lookup table for flow distribution control during dry days (where the rainfall is less than 25mm) to avoid the energy loss in the period. the calculation is shown in table 19.

Table 19 : Predicted financial gain for operation of intelligent controller in high and mid rainfall days for a year

Rainfall/day mm	**Additional generation /day kWh**	**Average occurrence days /year**	**CEB Feed in tariff LKR/kWh**	**Estimate gain LKR/year**
25mm-50mm	103	55	17.75	100,553.75
>50mm	1717	72		2,194,326.00
Annual Predicted Gain LKR				**2,294,879.75**

By looking at these figures, one can realize that even with the reduced energy harvest on dry days, the overall financial gain is at a considerable level when the power plant is operated with the intelligent controller due to its high gain on rainy days. And the financial gain is even higher if the power plant is adapted to a mixed operation procedure where the use of the intelligent controller is limited to the days where the rainfall is higher than 25mm.

But it is noteworthy that this prediction is done based on a simple calculation. A detailed prediction can be done by utilizing a statistical rainfall occurrence model [14] where the long-term catchment rainfall data from several stations will use as the model inputs. Also, the data for additional loss or gain in each rainfall period may vary depending on the duration of data collection.

6. CONCLUSION

- *There is a significant power loss due to river water quality variations in mini hydro power plants equipped with multiple turbines and long penstock lines which are fed by small streams.*
- *Major contributing facts to this power loss are the effects of micro particles and floating debris of the water.*
- *This issue can be mitigated by selecting the best operating points for each available river flow values (flow distribution combinations) based on current stream conditions and the selection can be done by looking at past operating data for the same flow condition.*
- *ANN is the most suitable intelligent controller tool which can utilize to update flow distribution table dynamically with the help of past data and current flow condition.*
- *The developed ANN based intelligent flow distribution controller provides improved power output for both clear water conditions and muddy water conditions.*
- *The average daily energy harvest of the power plant also improved with the developed intelligent controller.*
- *The developed intelligent controller can be used in any other power plant due to its generalized nature*
- *However, during dry periods this controller does not shows better performances when it comes to daily energy harvest. Therefore, conventional standalone turbine operation can be recommended for dry periods over this controller.*

7. FURTHER DEVELOPMENTS

This research output is produced with few limitations. Furthermore, some unaccounted data and methods also need to be analyzed to produce more accurate values. In this section, these areas are discussed.

7.1 Inclusion of automated rainfall data collection system

All the rainfall data used in this study is collected manually from a conventional rainfall gauge placed in the catchment area. Later during performance validation, the intelligent controller also fed with this manually collated rainfall data. This method is highly inconvenient for the powerplant operators to reach up to a far location in the catchment twice a day and get the rainfall reading manually.

Therefore, introducing an automated rain gauge capable of proved remote readings in a digital manner will improve the convenience of this controller. the said digital data can be directly linked to powerplant control computer which may result in improved controller performances and eligibility of collection of more training data as well.

7.2 Consider the accurate probability of rainfall occurrence during the validation

During the validation, it is noted that the designed intelligent controller does not suit dry days where the standalone turbine operation provides more energy harvest. However, the probability of occurrence of such dry days does not consider in this study.

It is noteworthy that the validity of the overall concept is highly dependent on the possibility of deployment of this controller throughout the year. Therefore, a separate study shall be carried out to check the probability of occurrence of such dry days throughout a year as mentioned in chapter 7.3. As per Sri Lanka's climate pattern, this validation may continue for a few years to predict an accurate probability of rainfall occurring during a given year [14] considering the fact that some years can be identified as extremely dry and wise versa.

7.3 Consideration of other unaccounted parameters as intelligent controller inputs.

This study is only limited to the effect of water quality parameters on power plant output reduction. There might be some other unaccounted parameters such as the present condition of the turbine (Present cavitation and surface condition), weather tightness of the labyrinth seal which will also contribute to the increase the power loss when water quality changes.

Therefore, such unaccounted parameters shall be considered in a further study and suitable data collection and analysis shall be performed. Also, if there is any relationship identified, those parameters shall be introduced to the intelligent controller as inputs in order to improve the performance of the intelligent controller.

7.4 Performance validation in other power plant

All the tastings and validations of this intelligent controller are limited to the Moragaha Oya Mini Hydropower plant. Since this controller is supposed to use as a universal solution, its performance shall be validated for other mini hydropower plants with multiple turbine setups, especially with different catchment characteristics and different climate patterns.

That way it is possible to verify that this solution can be used for any power plant without major modifications.

7.5 Study for economical viability

For any new technological improvement, there must be economical justification. The main goal of this development is to mitigate the experiencing power loss. But there is an initial capital expense that has to be incurred for the hardware and software. Apart from that, there is a considerable revenue loss due to the disturbances to the normal operation during the implementation period including the training data collection period. for this project to be economically viable, said expenses must be recovered by the income from the additional electricity generation obtained from the use of the intelligent controller in a justifiable time period.

That study has not been conducted during this research. Therefore, as a further study, a proper economical validation must be carried out for a number of cases.

Reference List

[1] Chyr Pyng LIOU," Limitations and Proper Use of the Hazen-Williams Equation" , American Society of Civil Engineers ,1998

[2] Alan V. Jopling , Donald L. Forbes, "Flume Study of Silt Transportation and Deposition", Geografiska Annaler: Series A, Physical Geography, Volume 61, 1979

[3] A. Wüest, G. Piepke and J.D. Halfman "Combined Effects of Dissolved Solids and Temperature on the Density Stratification of Lake Malawi", THE Limnology, Climatology and Paleoclimatology of the East African Lakes , 2019

[4] Sunita Singh , Arabinda Mishra "Spatiotemporal analysis of the effects of forest covers on stream water quality in Western Ghats of peninsular India", JOURNAL of Hydrology Volume 519, Part A, 27 November 2014

[5] Gerard V. Middleton , "Experiments on Density and Turbidity Currents", Canadian Journal of Earth Sciences, June 1967

[6] Jure Zupan," Introduction to Artificial Neural Network (ANN) Methods: What They Are and How to Use Them", Acta Chimica Slovenica, Volume 41,1994

[7] Khaled M. Matrouk, Haitham A. Alasha'ary, Abdullah I. Al-Hasanat, Ziad A. Al-Qadi, Hasan M. Al-Shalabi," Investigation and Analysis of ANN Parameters", European Journal of Scientific Research, Vol.121, 2014

[8] Anushka Perera, Upaka Rathnayake" Relationships between Hydropower Generation and Rainfall-Gauged and Ungauged Catchments from Sri Lanka", Mathematical Problems in Engineering, Volume 2020

[9] Miyuru B. Gunathilake , Chamaka Karunanayake, Anura S. Gunathilake, Niranga Marasingha,Jayanga T. Samarasinghe, Isuru M. Bandara, Upaka Rathnayake ," Hydrological Models and Artificial Neural Networks (ANNs) to Simulate Streamflow in a Tropical Catchment of Sri Lanka", Applied Computational Intelligence and Soft Computing,Volume 2021

[10] Lenore S. Clesceri, Arnold E. Greenberg, Andrew D. Eaton," Standard Methods for the Examination of Water and Wastewater": American Public Health Association 20th Edition, 2017

[11] MathWorks support documentation, "Linear and Nonlinear Regression", Version 2021

[12] Operation Manual, "TSW-30 Turbidity sensor", issue 2018

[13] F.Sanfilippo, "Introduction to Machine Learning and Big Data" : filipposanfilippo.inspitivity.com , 2019

[14] H.K.W.I. Perera , D.U.J. Sonnadara , D.R. Jayewardene , " Forecasting the Occurrence of Rainfall in Selected Weather Stations in the Wet and Dry Zones of Sri Lanka " , Sri Lankan Journal of Physics, Vol. 3 2002

[15] Ivan Nunes da Silva ,Danilo Hernane Spatti ,Rogerio Andrade Flauzino ,Luisa Helena Bartocci Liboni ,Silas Franco dos Reis Alves "Artificial Neural Networks" : Springer 2017

[16] Hira SinghSachdev ,Ashok KumarAkella ,NiranjanKumar , "Analysis and evaluation of small hydropower plants" : Renewable and Sustainable Energy Reviews , 2015

[17] R. V. Klyuev and I. I. Bosikov, "Research of water-power parameters of small hydropower plants in conditions of mountain territories," International Conference on Industrial Engineering, Applications and Manufacturing, 2016,

[18] Vineet Kumar Singh, S.K. Singal, "Operation of hydro power plants-a review", Renewable and Sustainable Energy Reviews, Volume 69, 2017

[19] Thiago BA Couto, Julian D Olden . "Global proliferation of small hydropower plants", Frontiers in Ecology and the Environment , 2018

Annex A – Code of intelligent controller

```
function varargout = GUI(varargin)

% GUI MATLAB code for GUI.fig

%      GUI, by itself, creates a new GUI or raises the existing

%      singleton*.

%

%      H = GUI returns the handle to a new GUI or the handle to

%      the existing singleton*.

%

%      GUI('CALLBACK',hObject,eventData,handles,...) calls the local

%      function named CALLBACK in GUI.M with the given input arguments.

%

%      GUI('Property','Value',...) creates a new GUI or raises the

%      existing singleton*.  Starting from the left, property value pairs are

%      applied to the GUI before GUI_OpeningFcn gets called.  An

%      unrecognized property name or invalid value makes property application

%      stop.  All inputs are passed to GUI_OpeningFcn via varargin.

%

%      *See GUI Options on GUIDE's Tools menu.  Choose "GUI allows only one

%      instance to run (singleton)".

%

% See also: GUIDE, GUIDATA, GUIHANDLES


% Edit the above text to modify the response to help GUI


% Last Modified by GUIDE v2.5 12-Nov-2020 12:42:25


% Begin initialization code - DO NOT EDIT

gui_Singleton = 1;

gui_State = struct('gui_Name',       mfilename, ...

                   'gui_Singleton',  gui_Singleton, ...

                   'gui_OpeningFcn', @GUI_OpeningFcn, ...

                   'gui_OutputFcn',  @GUI_OutputFcn, ...

                   'gui_LayoutFcn',  [] , ...

                   'gui_Callback',   []);
```

```
if nargin && ischar(varargin{1})
    gui_State.gui_Callback = str2func(varargin{1});
end

if nargout
    [varargout{1:nargout}] = gui_mainfcn(gui_State, varargin{:});
else
    gui_mainfcn(gui_State, varargin{:});
end
% End initialization code - DO NOT EDIT


% --- Executes just before GUI is made visible.
function GUI_OpeningFcn(hObject, eventdata, handles, varargin)
% This function has no output args, see OutputFcn.
% hObject    handle to figure
% eventdata  reserved - to be defined in a future version of MATLAB
% handles    structure with handles and user data (see GUIDATA)
% varargin   command line arguments to GUI (see VARARGIN)

% Choose default command line output for GUI
handles.output = hObject;
axes(handles.axes1);
load('eq.mat');
[X,Y] = meshgrid(0:0.5:100,0:0.5:100);
Z = eq(1,1) + eq(2,1)*X + eq(1,2)*Y + eq(3,1)*X.^2 + eq(2,2)*X.*Y + eq(1,3)*Y.^2 + eq(3,2)*(X.^2).*Y + eq(2,3)*(Y.^2).*X + eq(3,3)*(X.^2).*(Y.^2);
s=surf(X,Y,Z);
grid on;
zlabel('PP Output');
ylabel('FT2');
xlabel('FT1');
% Update handles structure

guidata(hObject, handles);
```

```
set(handles.tq1,'Value',1);

% UIWAIT makes GUI wait for user response (see UIRESUME)
% uiwait(handles.figure1);

% --- Outputs from this function are returned to the command line.
function varargout = GUI_OutputFcn(hObject, eventdata, handles)
% varargout  cell array for returning output args (see VARARGOUT);
% hObject    handle to figure
% eventdata  reserved - to be defined in a future version of MATLAB
% handles    structure with handles and user data (see GUIDATA)

% Get default command line output from handles structure
varargout{1} = handles.output;

% --- Executes on button press in pushbutton1.
function pushbutton1_Callback(hObject, eventdata, handles)
% hObject    handle to pushbutton1 (see GCBO)
% eventdata  reserved - to be defined in a future version of MATLAB
% handles    structure with handles and user data (see GUIDATA)

% --- Executes on button press in tq.
```

```
function tq_Callback(hObject, eventdata, handles)
% hObject    handle to tq (see GCBO)
% eventdata  reserved - to be defined in a future version of MATLAB
% handles    structure with handles and user data (see GUIDATA)

% Hint: get(hObject,'Value') returns toggle state of tq

global s;
s=serial('COM3','BaudRate',9600,'DataBits',8);
while get(hObject,'Value')
    pause(0.1);
    fopen(s);
    x = fscanf(s);
    fclose(s);
    y = str2double(x);
    if ~(isnan(y))
    set(handles.wq, 'string',y*20 );
    end
    pause(0.1);
end
if (~get(hObject,'Value'))
    fclose(s);
end
fclose(s);



% --- Executes on button press in pushbutton2.
function pushbutton2_Callback(hObject, eventdata, handles)
% hObject    handle to pushbutton2 (see GCBO)
% eventdata  reserved - to be defined in a future version of MATLAB
% handles    structure with handles and user data (see GUIDATA)
```

```
% --- Executes on button press in pushbutton3.

function pushbutton3_Callback(hObject, eventdata, handles)

% hObject    handle to pushbutton3 (see GCBO)

% eventdata  reserved - to be defined in a future version of MATLAB

% handles    structure with handles and user data (see GUIDATA)



% --- Executes on button press in run.

function run_Callback(hObject, eventdata, handles)

% hObject    handle to run (see GCBO)

% eventdata  reserved - to be defined in a future version of MATLAB

% handles    structure with handles and user data (see GUIDATA)

movegui(gcf,'center')

axes(handles.axes1);

c = [ 2 4 1; 7 9 -1; 0.2 2 5;] % output from the ANN

[X,Y] = meshgrid(0:0.5:100,0:0.5:100);

Z = c(1,1) + c(2,1)*X + c(1,2)*Y + c(3,1)*X.^2 + c(2,2)*X.*Y + c(1,3)*Y.^2 + c(3,2)*(X.^2).*Y + c(2,3)*(Y.^2).*X + c(3,3)*(X.^2).*(Y.^2);

s=surf(X,Y,Z);

grid on;

zlabel('PP Output');

ylabel('FT2');

xlabel('FT1');

%s(1,2)

T=['PP Output = ',num2str(c(1,1)),' + ',num2str(c(2,1)),'*FT1',' + ',num2str(c(1,2)),'*FT2',' + ',num2str(c(2,2)),'*FT1*FT2',' + ',num2str(c(3,1)),'*FT1^2',' + ',num2str(c(1,3)),'*FT2^2',' + ',num2str(c(3,2)),'*FT1^2*FT2',' + ',num2str(c(2,3)),'*FT1*FT2^2',' + ',num2str(c(3,3)),'*FT1^2*FT2^2'];

set(handles.eqtext, 'string',T ); % display outpu equation

% --- Executes when uibuttongroup3 is resized.

function uibuttongroup3_SizeChangedFcn(hObject, eventdata, handles)

% hObject    handle to uibuttongroup3 (see GCBO)

% eventdata  reserved - to be defined in a future version of MATLAB

% handles    structure with handles and user data (see GUIDATA)

%normalize the data
```

```
tinput=input';
toutput=output';
net = fitnet(15); % 10 hidden layer nurons
net.divideParam.trainRatio = 0.7;
net.divideParam.valRatio = 0.3;
net.divideParam.testRatio = 0;
net.trainParam.epochs = 10000;
[net,tr]=train(net , tinput , toutput);
%use net(input) to get the output
%check performances of output variable 1
moutput = net(tinput(:,:)); % model output
plot(moutput(1,:),toutput(1,:),'o');% plot model output variable 1,2 Vs actual output variable 1,2
hold on;
grid on;
%plot(moutput(2,:),toutput(2,:),'o');
hold off;
% RMS error 1st output variable
sqrt(mean((moutput(1,:)-toutput(1,:)).^2))
```

Annex B – Sample Training Data

Rainfall	Turbidity %	C0	C1	C2	C3	C4	C5	C6	C7	C8
24.8	84.7	0.356237	0.135149	0.747676	0.277262	0.607489	0.76408	0.559143	0.74557	0.01902
0.2	75.2	0.150291	0.43252	0.435566	0.731647	0.315779	0.084357	0.670779	0.644541	0.772703
19.8	40.8	0.606989	0.316205	0.745	0.111914	0.185858	0.503275	0.818015	0.872103	0.78893
5.2	21.2	0.220472	0.363134	0.118279	0.025956	0.393941	0.627226	0.816412	0.21166	0.989931
23.4	22.6	0.380142	0.987171	0.862332	0.636655	0.000105	0.957931	0.700514	0.837947	0.173
4.9	8.7	0.247763	0.790091	0.841527	0.616978	0.286472	0.990639	0.964007	0.247703	0.442717
15.4	84.2	0.274216	0.855269	0.47385	0.256565	0.662269	0.192618	0.582152	0.193148	0.282211
21.6	90.6	0.793486	0.070821	0.686986	0.628378	0.00964	0.18247	0.790537	0.496161	0.621188
0.7	43.3	0.502238	0.428297	0.596953	0.503794	0.283709	0.860852	0.486747	0.631713	0.372642
12.4	86.7	0.56946	0.560672	0.813627	0.50555	0.136075	0.988742	0.532309	0.350784	0.857347
7.3	51.3	0.618095	0.617202	0.601927	0.115848	0.334437	0.250251	0.677251	0.180594	0.796162
7.2	58.6	0.547294	0.78084	0.826442	0.4931	0.898704	0.812754	0.569135	0.111279	0.68989
3.1	47.0	0.887709	0.753829	0.728751	0.084558	0.784577	0.136072	0.888228	0.359626	0.935593
10.8	87.2	0.619552	0.783329	0.553167	0.271332	0.275172	0.013756	0.060373	0.726237	0.792212
8.4	33.3	0.109241	0.033376	0.357217	0.911313	0.602262	0.293569	0.337194	0.87389	0.829325
2.2	55.4	0.834837	0.671083	0.0488	0.209099	0.835741	0.596047	0.030413	0.504124	0.065408
3.3	4.2	0.292283	0.963497	0.125772	0.224079	0.759695	0.755011	0.210648	0.241552	0.61105
6.4	96.9	0.959598	0.645188	0.853592	0.433095	0.295514	0.177876	0.837415	0.119551	0.188885
5.9	28.1	0.393436	0.356122	0.455907	0.886508	0.431144	0.543407	0.591251	0.702193	0.072907
22.9	25.9	0.899083	0.073266	0.841868	0.497347	0.838948	0.901629	0.440627	0.751422	0.131746
3.9	7.2	0.899119	0.738098	0.78494	0.279177	0.290739	0.500344	0.665967	0.720375	0.431061
19.2	83.1	0.6536	0.903807	0.654355	0.919935	0.318895	0.333351	0.048912	0.163185	0.205197
18.7	12.7	0.578587	0.135039	0.379281	0.510506	0.097287	0.829011	0.799165	0.143714	0.71127
17.9	15.4	0.014951	0.08783	0.014494	0.99402	0.263913	0.960619	0.312457	0.380701	0.594943
24.9	40.1	0.685251	0.079253	0.671528	0.376596	0.09898	0.785868	0.806653	0.129361	0.822113
0.6	12.0	0.776602	0.517794	0.8051	0.119564	0.263042	0.833011	0.909	0.734399	0.083409
6.2	24.7	0.982853	0.224207	0.240953	0.860242	0.623725	0.055113	0.914413	0.19212	0.258518
13.4	7.2	0.738736	0.014387	0.025176	0.636104	0.897155	0.737639	0.161201	0.223713	0.300398
8.5	9.0	0.873305	0.868466	0.651723	0.051312	0.516519	0.602788	0.01663	0.126133	0.757751
16.9	27.3	0.682314	0.921506	0.653917	0.37903	0.01748	0.567067	0.982576	0.92369	0.064553
13.2	6.4	0.089226	0.936915	0.110361	0.665873	0.843865	0.849201	0.049792	0.937929	0.616907
13.8	67.0	0.825157	0.344605	0.556075	0.167322	0.39779	0.880605	0.326964	0.177289	0.996034
8.7	28.5	0.210052	0.680383	0.300533	0.813647	0.922674	0.280647	0.506731	0.579999	0.466074
5.9	36.3	0.054527	0.364925	0.814506	0.650617	0.324748	0.91585	0.151711	0.084761	0.328446
3.2	61.7	0.59029	0.638029	0.193161	0.34101	0.416927	0.118237	0.050762	0.878878	0.011696
16.4	32.1	0.507191	0.826667	0.63954	0.798409	0.38466	0.053679	0.236419	0.248089	0.679933
7.5	14.1	0.211116	0.53452	0.420488	0.411455	0.674894	0.519922	0.74626	0.55193	0.059964
14.3	27.2	0.144162	0.322762	0.641184	0.167168	0.961744	0.043047	0.487546	0.118115	0.705574
15.9	20.3	0.681745	0.416788	0.94734	0.348254	0.426448	0.225862	0.910721	0.311436	0.084955
14.8	38.7	0.531875	0.534217	0.494463	0.923249	0.382332	0.689233	0.359876	0.725191	0.041802
12.6	99.6	0.563536	0.155467	0.020329	0.533843	0.275415	0.856067	0.619253	0.437307	0.686156
13.9	42.5	0.302658	0.981338	0.663963	0.013434	0.676197	0.927984	0.541221	0.244606	0.916512

5.9	2.8	0.724766	0.311405	0.131693	0.224952	0.355542	0.329469	0.445219	0.00507	0.398938
19.8	33.4	0.190391	0.408426	0.130038	0.168995	0.602694	0.730968	0.258479	0.210914	0.233684
24.3	99.2	0.99491	0.869676	0.792183	0.539485	0.528113	0.044167	0.379262	0.485123	0.245489
4.8	93.8	0.887147	0.340162	0.48077	0.833637	0.183567	0.382436	0.113004	0.352009	0.264685
5.8	37.0	0.121611	0.009	0.754482	0.570662	0.744214	0.212448	0.668849	0.743821	0.598621
7.4	30.3	0.52278	0.214738	0.595246	0.914871	0.178186	0.546417	0.405409	0.362764	0.530033
19.5	61.7	0.744746	0.100592	0.609809	0.375422	0.715265	0.251762	0.285846	0.28139	0.080035
6.7	6.4	0.047521	0.228776	0.330432	0.288003	0.613693	0.413876	0.087113	0.92713	0.262642
7.5	34.5	0.03925	0.104085	0.134638	0.884647	0.456534	0.560409	0.543354	0.264433	0.473761
9.7	41.8	0.484394	0.419188	0.211522	0.691173	0.945057	0.335381	0.846871	0.022303	0.30819
19.7	34.2	0.124329	0.955134	0.286176	0.295704	0.932884	0.365165	0.16052	0.570664	0.880894
7.8	27.5	0.90581	0.885232	0.321732	0.634307	0.210896	0.663653	0.268397	0.353178	0.194562
6.3	19.5	0.818624	0.378192	0.828927	0.530041	0.448155	0.310017	0.592329	0.591717	0.919863
22.3	33.4	0.558901	0.311307	0.10591	0.60339	0.849807	0.479748	0.778567	0.228708	0.098591
4.3	72.0	0.294616	0.787196	0.184682	0.873082	0.268091	0.924533	0.932658	0.79853	0.660158
8.9	49.2	0.220545	0.328667	0.140368	0.986607	0.695223	0.211284	0.968801	0.676849	0.911715
18.0	40.5	0.748899	0.082914	0.82011	0.189369	0.170011	0.919371	0.105735	0.292262	0.552775
9.4	89.1	0.974796	0.600943	0.02953	0.046578	0.980568	0.250586	0.422871	0.713691	0.912161
10.8	33.7	0.681766	0.050291	0.843553	0.215419	0.237325	0.594596	0.482417	0.372224	0.906572
0.6	48.1	0.695692	0.816457	0.216321	0.625192	0.697349	0.952956	0.952409	0.908691	0.303742
9.5	2.7	0.910431	0.109417	0.305173	0.110907	0.672143	0.76206	0.435015	0.620742	0.9272
22.8	83.3	0.256665	0.811352	0.202551	0.664597	0.51256	0.501633	0.780267	0.829788	0.509814
22.1	78.1	0.283386	0.358596	0.311146	0.457056	0.697072	0.653336	0.318215	0.033585	0.181144
17.0	49.9	0.890564	0.75967	0.485058	0.081994	0.842343	0.476323	0.031707	0.42237	0.535347
11.6	94.5	0.150098	0.215815	0.931593	0.256816	0.59347	0.366012	0.121754	0.735829	0.0637
5.4	53.8	0.52963	0.636166	0.739264	0.800965	0.290282	0.507084	0.18268	0.45678	0.256965
6.2	10.2	0.630013	0.187131	0.58879	0.381482	0.027829	0.25799	0.133079	0.769071	0.182768
17.8	39.7	0.568322	0.497578	0.668038	0.624937	0.045534	0.026489	0.911273	0.109621	0.22748
3.7	64.6	0.24538	0.511956	0.151559	0.129351	0.654497	0.546037	0.398744	0.015056	0.955055
13.4	27.0	0.418258	0.073219	0.468549	0.436816	0.337099	0.670464	0.068367	0.760757	0.768308
21.9	26.2	0.094042	0.73131	0.863386	0.574669	0.575954	0.300546	0.166582	0.266325	0.976664
1.8	96.6	0.92317	0.919563	0.870973	0.618576	0.222003	0.523441	0.546916	0.540194	0.342306
18.1	6.9	0.341917	0.561172	0.277921	0.920224	0.598243	0.441118	0.244128	0.304603	0.367935
12.4	48.0	0.23242	0.227603	0.010081	0.75192	0.729412	0.718252	0.636794	0.041652	0.563264
17.2	65.6	0.094976	0.37969	0.53181	0.953661	0.706228	0.743598	0.64599	0.850346	0.298477
0.8	45.2	0.458014	0.643624	0.641893	0.771096	0.202423	0.488992	0.733324	0.576335	0.907058
16.9	67.4	0.176547	0.584227	0.230567	0.226759	0.843167	0.219162	0.947687	0.379584	0.763161
11.1	55.5	0.432586	0.959587	0.050773	0.028505	0.486185	0.658403	0.350849	0.597828	0.496416
19.6	99.0	0.449965	0.604663	0.610752	0.196345	0.650093	0.631331	0.221671	0.926375	0.957085
9.2	59.1	0.209379	0.65114	0.756249	0.554183	0.453052	0.938531	0.394348	0.280567	0.259362
16.1	86.8	0.171204	0.01434	0.90857	0.386235	0.412493	0.694436	0.303429	0.90372	0.557206
13.8	23.5	0.842897	0.047358	0.364805	0.827983	0.377046	0.877107	0.209965	0.332447	0.030122
3.8	21.9	0.803164	0.197653	0.710982	0.258577	0.644576	0.652723	0.341187	0.076599	0.005384
2.0	79.4	0.278086	0.417617	0.511882	0.583707	0.555554	0.594627	0.129158	0.411969	0.524968
11.4	75.8	0.392177	0.182046	0.111739	0.199113	0.514003	0.781085	0.424809	0.728845	0.132837
13.2	79.3	0.044154	0.620388	0.082641	0.568886	0.369824	0.184096	0.372412	0.99927	0.728493

13.5	20.8	0.783888	0.524854	0.242704	0.204001	0.463998	0.456182	0.998641	0.145153	0.305475
0.2	74.1	0.685641	0.887164	0.509288	0.804982	0.753285	0.92225	0.135037	0.281354	0.985035
23.6	46.9	0.863604	0.783765	0.796649	0.902109	0.294473	0.844049	0.463108	0.29601	0.708524
14.1	62.1	0.431842	0.251033	0.513417	0.929817	0.434076	0.88475	0.422458	0.023247	0.249464
17.0	81.0	0.54046	0.207111	0.713836	0.7446	0.386172	0.554741	0.120334	0.500875	0.962533
13.2	62.6	0.130526	0.809574	0.033084	0.045456	0.772251	0.841193	0.402331	0.786333	0.935832
18.7	35.9	0.689368	0.291209	0.844511	0.633185	0.391351	0.085008	0.845657	0.98115	0.39216
18.9	27.2	0.749957	0.297268	0.323039	0.021457	0.137034	0.23984	0.101781	0.863011	0.820995
13.8	36.9	0.54925	0.831743	0.135057	0.010204	0.883866	0.693293	0.935776	0.972336	0.374112
0.4	59.6	0.274971	0.084666	0.851289	0.546027	0.717745	0.025038	0.480694	0.531784	0.049092
22.1	77.4	0.507941	0.481135	0.531612	0.994147	0.998765	0.547551	0.522038	0.415625	0.472632
9.1	46.7	0.472285	0.074375	0.330131	0.010447	0.54946	0.339021	0.570675	0.29149	0.888952